
COMMENCING-STUDENT ENROLMENT FORECASTING UNDER DATA SPARSITY WITH TIME SERIES FOUNDATION MODELS

A PREPRINT

 **Jittarin Jetwiriyanon***

School of Mathematical and Computational Sciences
Massey University
Albany, New Zealand

 **Teo Susnjak†**

School of Mathematical and Computational Sciences
Massey University
Albany, New Zealand

 **Surangika Ranathunga‡**

School of Mathematical and Computational Sciences
Massey University
Albany, New Zealand

February 13, 2026

ABSTRACT

Many universities face increasing financial pressure and rely on accurate forecasts of commencing enrolments. However, enrolment forecasting in higher education is often data-sparse; annual series are short and affected by reporting changes and regime shifts. Popular classical approaches can be unreliable, as parameter estimation and model selection are unstable with short samples, and structural breaks degrade extrapolation. Recently, TSFMs have provided zero-shot priors, delivering strong gains in annual, data-sparse institutional forecasting under leakage-disciplined covariate construction. We benchmark multiple TSFM families in a zero-shot setting and test a compact, leakage-safe covariate set and introduce the Institutional Operating Conditions Index (IOCI), a transferable 0-100 regime covariate derived from time-stamped documentary evidence available at each forecast origin, alongside Google Trends demand proxies with stabilising feature engineering. Using an expanding-window backtest with strict vintage alignment, covariate-conditioned TSFMs perform on par with classical benchmarks without institution-specific training, with performance differences varying by cohort and model.

Keywords student forecasting, time series foundation models, time series forecasting, zero-shot forecasting, multivariate forecasting, forecasting with covariates

1 Introduction

Accurate forecasts of new-student enrolments and the annual intake of students commencing study are central to strategic and operational planning in higher education institutes. Staffing profiles, teaching capacity, residential provisioning, and tuition-revenue outlooks all depend on credible forward views of year-ahead new-student intake volumes [1, 2]. The need for dependable enrolment forecasting has intensified as universities operate under tightening financial constraints [3] and face looming demographic shifts. For example, in the United States, the approaching enrolment cliff is expected to reduce the college-aged population, largely reflecting birth-rate declines during the Great Recession [4]. At the same time, continued economic volatility has accelerated pre-existing patterns of financial fragility, increasing the reliance on data-driven forecasting to manage deficits and support resource allocation [5, 6]. In such conditions, static historical averaging is increasingly inadequate; institutions require dynamic forecasting frameworks to support sustainability [7] as competition for public resources intensifies and cost pressures persist [8, 9]. In these environments, extrapolative

* Corresponding author: jittarin.jetwiriyanon.1@uni.massey.ac.nz

† Contributing author: T.Susnjak@massey.ac.nz

‡ Contributing author: S.Ranathunga@massey.ac.nz

approaches and ratio-based projection methods whose validity depends on local persistence can fail sharply at turning points [10].

A further difficulty is that institutional enrolment series are often short, aggregated, and privacy-constrained [11, 12]. Annual reporting is common, and even when multi-year administrative histories exist, the number of effective training observations can be small once cohort definitions, reporting changes, and structural breaks are accounted for. Under these low signal-to-noise conditions, persistence-style baselines can remain competitive beyond very short horizons, while richer classical models become unstable or overfit unless they are anchored by credible exogenous structure [13]. These constraints motivate multivariate, context-aware forecasting approaches that can incorporate externally observable drivers while preserving privacy, operational simplicity, and the temporal discipline required for deployable decision support [14].

Recent TSFMs offer a promising pathway for forecasting in data-sparse institutional settings [15, 16, 17, 18]. Pre-trained on large, heterogeneous corpora, TSFMs can provide strong zero-shot priors and, in many cases, support conditioning on dynamic covariates without institution-specific fine-tuning [18, 17]. This property is attractive where data sharing is limited but external indicators remain informative. Nevertheless, evidence remains limited on whether covariate-conditioned, zero-shot TSFMs can reliably outperform well-specified classical baselines for student enrolment forecasting at an annual frequency [19]. Practical guidance is also scarce on how to construct leakage-safe covariates under sparsity, when covariates will help versus destabilise model behaviour [14].

Accordingly, public web signals provide a pragmatic source of external covariates by injecting structure that is not always visible in the target series. Search-intensity measures can proxy latent demand and public attention, while text- and event-based information can be compressed into low-dimensional indicators that summarise shifts in the wider operating environment [20]. However, these signals must be engineered conservatively to avoid leakage and spurious fit [14]. In data-sparse settings, disciplined decision-time covariate construction is essential: covariates must add exogenous information without contaminating the forecast origin. Because search-platform indices are normalised within each extraction window and may vary across extractions, robust practice requires explicit vintage control, aggregation to the decision frequency, and stabilising transformations that reduce sensitivity to re-scaling and re-indexing [21].

The same discipline is required for richer, unstructured sources, where the challenge of converting unstructured external information into leakage-safe covariates follows a text-as-data perspective, treating narrative documents as quantitative evidence rather than purely descriptive context [22]. In practice, this means defining a transparent coding scheme that maps time-stamped text into numerical features such as sentiment, topic prevalence, constraint intensity and then aggregating these signals to the frequency. Conceptually, this approach is analogous to established text-derived uncertainty indices that translate qualitative narratives into interpretable time series by counting, classifying, and aggregating uncertainty related in documents [23]. Those movements in the resulting covariate reflect genuine changes in the operating environment rather than inadvertent incorporation of future knowledge.

The potential of TSFMs can operationalise unstructured environmental information without expensive institution-specific fine-tuning and provide higher-education institutions with a dynamic tool for anticipating structural breaks. Moving beyond purely extrapolative baselines toward a multivariate, context-aware forecasting regime offers the strategic foresight required to navigate demographic headwinds and financial volatility in modern higher education.

Contribution

This paper provides an operational evaluation of annual commencing-enrolment headcounts, assessing zero-shot TSFMs for institutional forecasting under severe data sparsity. Using expanding-window backtesting with strict covariate vintage control, we benchmark multiple TSFM families against classical baselines, under both unconditioned (no-covariate) and covariate-conditioned settings using Google Trends demand proxies and an IOCI. In sparse annual histories, covariate-conditioned TSFMs can be competitive with classical baselines and, in several configurations, reduce point-forecast error. However, covariate effects are heterogeneous. The same signal may improve one model family while destabilising another, underscoring the complexity of model selection under non-stationarity. The study concludes with a year-by-year audit trail, designed to serve as a transferable framework for universities seeking to integrate these contextual signals.

- **A benchmark for annual enrolment:** We benchmark zero-shot TSFMs for year-ahead new-entrant forecasting on domestic and international cohorts, using an expanding-window backtest where all covariates are lagged and vintage-aligned to each forecast origin, and compare against classical baselines.

- **Model covariate compatibility under data sparsity:** We characterise when conditioning helps versus destabilises by tracking point accuracy and uncertainty quality across cohorts and model families, separating robust improvements from brittle behaviour that arises with short annual histories.
- **Auditable covariate protocol and portable context signal:** We provide a leakage-disciplined covariate and introduce IOCI and Google Trends as transferable operating-conditions covariates with a year-by-year evidence trail that can be reproduced and audited.

2 Related Work

2.1 Enrolment forecasting under institutional constraints

Early methods for enrolment projection were predominantly univariate. Techniques like grade-progression ratios and cohort-survival calculations were widely used in the 1970s–1990s for school and college planning, relying on recent flows between grades to extrapolate forward [24]. Alongside these deterministic heuristics, simple time series baselines such as the persistence naïve forecast, which sets the next value equal to the most recent level, were common because they are easy to compute and surprisingly hard to beat over very short horizons [25]. By the 2000s, attention shifted to multivariate statistical models that handle multiple drivers. ARIMA and exponential-smoothing variants were applied to enrolment series with mixed results, reflecting differences in series properties and settings. Critically, ARIMAX and state-space formulations allow the incorporation of exogenous predictors and time-varying components without rebuilding models from scratch [26, 27]. This direction mirrors broader macro-forecasting practice, where data fusion and factor model ideas are standard to cope with low signal-to-noise environments [28]. National projections similarly combine enrolments with population and economic covariates [29].

2.2 Covariates in student enrolments

Forecasting new student enrolments is a multifaceted challenge that benefits from a wide lens on potential predictors. Incorporating direct covariates [30] can capture the complex drivers behind enrolment trends from public web signals such as Google Trends and signals [20, 31, 23, 32]. Traditional factors like demographic shifts and economic indicators remain fundamental. For example, knowing the number of high school graduates or the state of the job market provides a grounded expectation for enrolment changes [33]. At the same time, data sources such as digital search trends and mobility data offer a cutting-edge complement, often providing early warnings of shifts in student interest that appear in historical enrolment data [34]. The integration of these diverse covariates marks a shift from static, trend-extrapolation models to dynamic, responsive forecasting approaches that condition on exogenous drivers. The choice of proxy variable as covariates will depend on the context. Successful forecasting models in higher education often iterate and test which covariates add predictive power, sometimes using feature selection to focus on the most impactful ones [35].

2.3 Feature engineering for covariates

Despite advances in model architectures, feature engineering remains vital in both conventional and modern forecasting. Creating informative transformations of the raw sequence often boosts accuracy even for deep and transformer-based models that incorporate covariates [36]. A fundamental example is the lag feature for annual data, the one-year lag is $\ell_t^{(1)} = x_{t-1}$; for sub-annual data with m observations per year, it generalises to $\ell_t^{(1)} = x_{t-m}$. This covariate injects short-run persistence while avoiding look-ahead when computed within the training window. Another important class are window summary statistics that condense recent history moving averages and exponential smoothing reducing noise and highlight trends. With m observations per year, a two-year exponentially weighted Moving Average uses span $S = 2m$ and a three-year EWMA uses span $S = 3m$ in the standard recursion [37]. Likewise, multi-year simple moving averages smooth year-to-year volatility so the model can focus on the stable component. Many modern architectures explicitly allow static and time-varying covariates, and performance can hinge on thoughtful covariate engineering and selection [38].

2.4 LLMs for institutional narratives and stress signals

Recent advances in large language models (LLMs) such as GPT, Gemini, and Claude variants have made rubric-based text coding feasible in settings where task-specific labelled data are scarce [39]. A growing evaluation literature shows that modern LLMs can match and in some tasks exceed traditional human-coding pipelines for annotation and survey-response coding [40]. LLMs are increasingly used to operationalise institutional narratives into structured, time-indexed indicators of stance, risk, and operating stress [41]. For instance, large-scale work on central bank communications applies LLM classifiers at the sentence level to extract multidimensional signals from a multilingual historical corpus,

and then aggregates these outputs into interpretable indices and crisis-sensitive risk signals [42]. Such designs provide a close analogue to text-derived operating-conditions covariates, narrative evidence is converted into a time series that can be aligned to decision time, compared across periods, and validated via external outcomes [43, 44]. Best practice also emphasises retrospective verification, stability checks across prompt variants, and transparent documentation [22].

2.5 Zero-Shot TSFMs with covariates in student enrolment forecasting

A major development in time series forecasting is the rise of TSFMs, large pre-trained models designed to serve as general purpose forecasters across domains [45] (Figure 1). These models, inspired by the success of Large Language Models, are trained on massive collections of time series data and can perform forecasting in a zero-shot manner [46, 47]. Several notable TSFMs have emerged, Moirai from Salesforce [18, 48], TimesFM from Google [17, 49], and Chronos-Bolt from AWS [16, 50, 51]. Many TSFMs can incorporate covariates by receiving them as additional input channels alongside the target history. In masked-encoder architectures, dynamic covariates can be provided as parallel variates within the input sequence, enabling the attention mechanism to condition forecasts on external signals [52, 16]. This capability is attractive for student enrolment forecasting, where institutional histories are short, and privacy constraints limit task-specific training. The convergence of TSFMs and domain-specific covariates offers a promising path for student enrolment forecasting, particularly in the common scenario of limited and scarce institutional data.

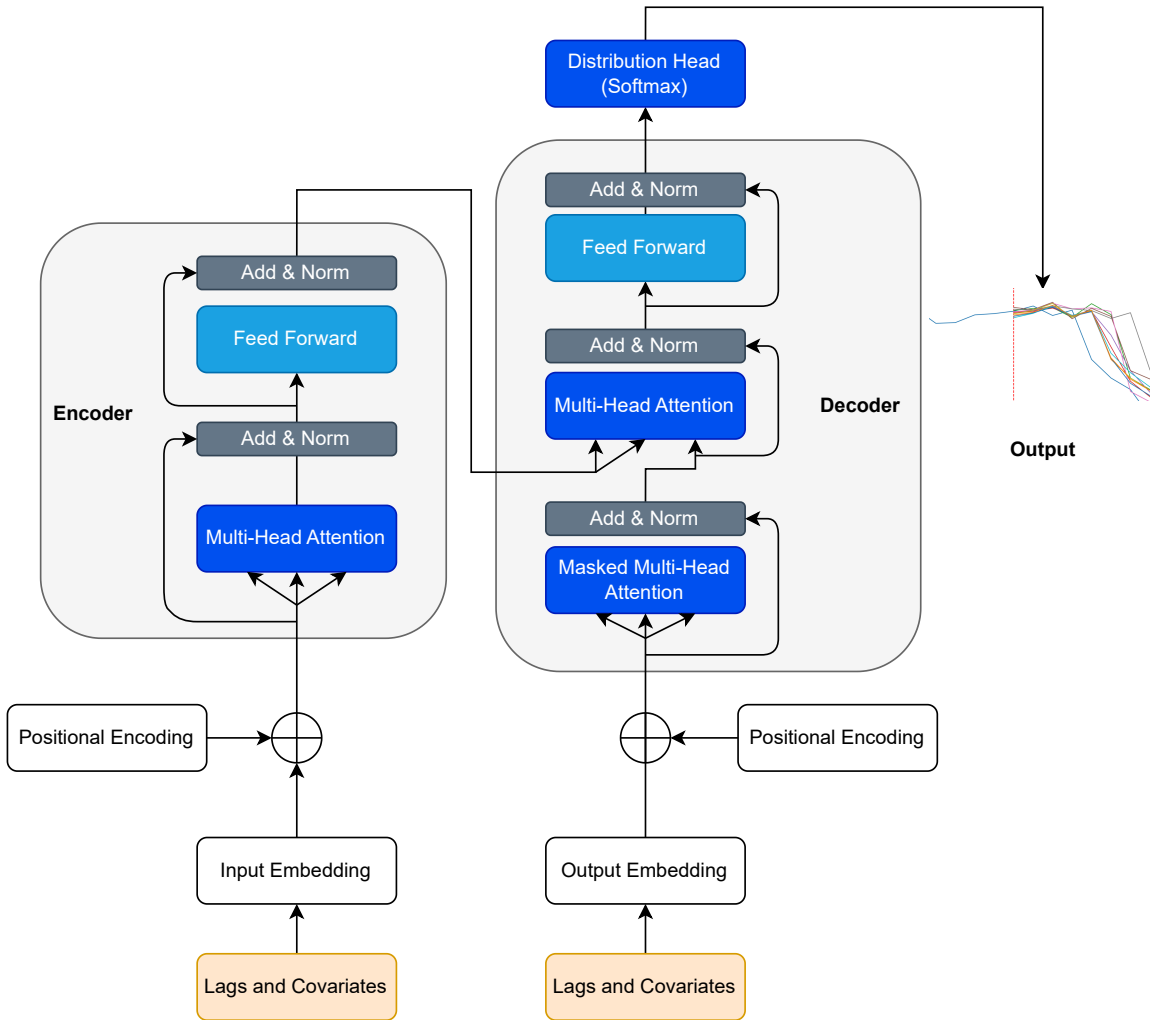


Figure 1: Time series foundation model architecture for multivariate time series forecasting [53].

2.6 Summary and research questions

TSFMs have demonstrated strong zero-shot capabilities across diverse public benchmarks, evidence remains limited regarding their reliability in data-sparse institutional settings governed by strict leakage controls. Furthermore, although external signals offer improved forecasting potential, their inherent sampling variability can render naive implementations unstable. To address these gaps, this study benchmarks pretrained TSFMs against strong classical baselines within a leakage-safe framework. Specifically, we evaluate whether TSFMs, when combined with leakage-disciplined covariates, yield reproducible gains in both point accuracy and probabilistic calibration for annual enrolment planning. To address these challenges, this study investigates the following research questions:

- **RQ1** To what extent do zero-shot TSFMs outperform strong classical baselines for *annual new-entrant enrolment* forecasting under institutional data sparsity?
- **RQ2** Under annual sampling and severe sparsity, when do *leakage-safe* external covariates *help versus destabilise* zero-shot TSFMs, and how does this vary with model family and capacity?
- **RQ3** Which covariate constructions and feature-engineering choices yield *robust and reproducible* improvements in accuracy and probabilistic calibration, and which choices are brittle?

3 Methodology

3.1 Dataset

We evaluated the proposed forecasting pipeline on annual commencing student headcounts (new enrolments) extracted from Massey University’s administrative enrolment system, as a data-sparse institutional planning setting, disaggregated into domestic and international cohorts. Although the study is conducted at a single university, the contribution fits a transferable workflow for forecasting in data-sparse institutions. The outcome was treated as an administrative headcount of new entrants, consistent with institutional reporting practice. Pre-processing was intentionally minimal. We harmonised cohort definitions across years and applied adjustments for consistency. Where historical reporting introduced minor rounding or reconciliation discrepancies, we permitted a small numerical tolerance in validation checks while retaining the original measurement scale. The dataset comprises two annual target series domestic and international commencing-enrolment headcounts spanning 2007–2025 (19 annual observations per series), which form the target variables for evaluation.

3.1.1 Feature engineering for Google Trends

Google Trends web signals were extracted using a consistent query term (*Massey University*) over worldwide and domestic search geographies. We followed a standardised extraction procedure where the institution’s name serves as the query anchor, allowing for consistent replication across different entities [54]. We extracted Google Trends relative search volume (RSV) for the worldwide query. RSV is scaled to 0-100 within each extraction window and reflects relative popularity rather than absolute search counts. We aggregated monthly RSV to annual summaries aligned with the enrolment decision frequency, standardised within each training window, and constructed leakage-safe features commonly used as demand proxies [55].

Feature engineering for covariates Engineered summaries were used to improve stability when covariates were supplied to forecasting models. Let $\{x_t\}_{t=1}^T$ denote the annual scalar input series used to construct a covariate, indexed by year t . Let $m_t^{(s)}$ denote an exponentially weighted moving average (EWMA) of x_t with span parameter s in years and smoothing factor $\alpha_s \in (0, 1]$. We used the common span parameterisation $\alpha_s = \frac{2}{s+1}$, and initialise the recursion with $m_1^{(s)} = x_1$.

Exponentially weighted moving average (2-year) The 2-year EWMA smoothed short-run noise while retaining recent movements. Using the common span parameterisation, $\alpha_s = \frac{2}{s+1}$, we set $\alpha_2 = \frac{2}{3}$ and defined the recursion in Equation 1.

$$m_t^{(2)} = \alpha_2 x_t + (1 - \alpha_2) m_{t-1}^{(2)}, \quad m_1^{(2)} = x_1 \quad (1)$$

Compared with a simple moving average, the EWMA places greater weight on recent observations, allowing it to adapt faster to level shifts.

Exponentially weighted moving average (3-year) A slightly smoother variant emphasised the medium-run signal with reduced volatility. With $\alpha_3 = \frac{2}{4} = \frac{1}{2}$, we defined Equation 2.

$$m_t^{(3)} = \alpha_3 x_t + (1 - \alpha_3) m_{t-1}^{(3)}, \quad m_1^{(3)} = x_1 \quad (2)$$

Relative to EWMA2, this covariate was less reactive but more noise-robust.

Lag-1 level To inject short-run persistence as an exogenous predictor, we included the lag-1 level in Equation 3.

$$\ell_t^{(1)} = x_{t-1}, \quad t \geq 2. \quad (3)$$

3.1.2 Operationalisation of institutional operating conditions

We specify a reproducible procedure for constructing IOCI as a template for converting time-stamped institutional narrative evidence into a comparable regime covariate. Using a fixed prompt schema and scoring rubric (Appendix A), an LLM maps the year- t evidence pack into a consistent 0-100 measure of operating pressure, yielding an annual scalar $\text{IOCI}_t \in [0, 100]$. Where necessary for interpretation, the model may consult reputable public context explicitly dated to the scored year, but the score and justification must remain anchored to the supplied institutional evidence. Unlike economy-wide uncertainty measures, IOCI is designed as an institution-level, decision-time covariate for enrolment forecasting; evidence is restricted to information available for year t and explicit vintage constraints are enforced to prevent look-ahead bias.

Although the IOCI evidence often referenced international enrolment fee dependency, the construct was designed to reflect institution-wide operating conditions. In many university systems, international fee income cross-subsidises domestic teaching and broader institutional activity, so shocks to international income are transmitted directly into domestic-facing operations. This made the signal plausibly predictive for domestic enrolment outcomes as well.

To make the procedure practical and repeatable, we wrote a dedicated system prompt that specified the analyst role, the scoring scale, and explicit constraints on evidence use. The prompt framed (B) the model as a university planning/administrative analyst and instructed it to rate operating stress on a 0-100 scale based only on the supplied text. We also built guardrails into the process, including year-specific scoring, avoidance of assumptions when evidence was unclear, and explicit rationales linking evidence to scores. In this way, the process remained transparent and replicable, and the prompt itself constituted a reusable contribution for other institutional settings.

Table 1 shows a retrospective verification of the IOCI construction procedure by four LLM configurations Grok Fast 1, Gemini 3 Pro, Claude Opus 4.5, and GPT-5.2 Thinking. Specifically, we applied the fixed prompt to the historical, year-indexed evidence and compared the resulting model-derived IOCI scores against an existing reference series. Concordance between the two series provides supporting evidence that the prompt operationalises the intended construct and yields a reproducible mapping from narrative evidence to a quantitative regime covariate. The calibrated IOCI series treats the GPT-5.2 Thinking configuration outputs as the primary signal and applies a bounded post-hoc adjustment (± 1 point) to improve level alignment. This calibration is intentionally conservative, it preserves the year-to-year ordering while correcting minor systematic offsets and reducing small inconsistencies attributable to stochastic variation in model judgements.

Table 1: Model-generated series by year.

Year	Grok Fast 1	Gemini 3 Pro	Claude Opus 4.5	GPT 5.2 Thinking	Calibrated
2007	8	10	12	15	15
2008	8	10	12	15	15
2009	8	10	12	15	15
2010	17	19	17	20	21
2011	13	14	14	6	7
2012	14	15	16	7	6
2013	14	15	16	7	7
2014	53	46	48	48	49
2015	55	49	50	51	51
2016	57	50	52	53	54
2017	29	35	38	39	39
2018	59	47	50	50	51
2019	57	55	57	57	58
2020	95	86	92	85	86
2021	94	90	95	95	95
2022	92	88	90	94	94
2023	71	75	73	74	75
2024	50	58	55	58	59
2025	30	38	35	39	39

3.2 Zero-shot forecasting with covariate

We utilised zero-shot TSFMs to generate enrolment forecasts while keeping all model weights fixed. In this setting, the pre-trained model served as a strong domain prior learned from large and heterogeneous collections of time series. This strategy was well-suited to institutional contexts with short histories and privacy constraints, because it avoided dataset-specific training while enabling the use of external signals without exposing individual-level records.

Let y_t denote annual new-enrolment counts for each cohort. We assembled a covariate matrix \mathbf{X}_t comprising internal administrative indicators, public attention proxies, and structural features available at the forecast origin. Missing values were imputed via last-observation-carried-forward for observed-history features and via known-future encodings for design-time features. For each forecast origin t in an expanding-window backtest, we passed a multivariate context of length L :

$$\mathcal{C}_t = \{(y_{t-L+1}, \mathbf{X}_{t-L+1}), \dots, (y_t, \mathbf{X}_t)\}.$$

For TSFMs that supported dynamic covariates over the forecast horizon H , we supplied covariate history up to t only; no future values were injected in the reported results. When scenario analysis was of interest, future covariate paths could be supplied to obtain counterfactual forecasts.

3.3 Baseline models

We provided interpretable references to quantify the incremental value of the proposed forecasting experiments. These baselines clarified what performance was achievable under a stringent evaluation threshold.

3.3.1 Persistence

The persistence benchmark projected the last observed value forward across all forecast horizons, repeating the carried-forward level over the entire window [56]. Despite its simplicity, persistence was often competitive in short samples and served as a conservative lower bound for acceptable performance; evidence from large-scale forecasting competitions showed that simple benchmarks could rival more complex methods, especially around structural change and limited data [13]. Persistence was particularly appropriate for series that were well-approximated by a random walk, where the optimal multi-step predictor equalled the most recent observation and more elaborate techniques could not systematically outperform the naïve forecast [57]. Recent applications also documented the practicality of persistence-style baselines in operational settings [25]. Consequently, persistence provided a realistic baseline for assessing genuine predictive value from more complex models. Given a series $\{y_t\}_{t=1}^T$ and horizon H , the persistence (naive) forecast carried the last observed level forward:

$$\hat{y}_{t+h|t} = y_t, \quad h = 1, \dots, H. \quad (4)$$

3.4 ARIMA

We adopted ARIMA as the classical baseline [58], fitting non-seasonal forms on each training window and allowing exogenous regressors (ARIMAX) composed of selected lagged terms [59]. Multi-step forecasts were generated recursively, and all parameters were re-estimated at each expanding origin to accommodate evolving dynamics and mitigate parameter drift [60]. Model adequacy was routinely checked via residual whiteness and stability to ensure that comparisons against foundation models rested on well-specified baselines [61]. We estimated non-seasonal ARIMAX(p, d, q) parameters by exact maximum likelihood, using concentrated intercept and innovation variance where appropriate [62]. Prediction intervals were derived from the linear forecast error variance obtained via the innovations algorithm; these intervals relied on second-order properties, with normal or bootstrap approximations applied where residuals deviated from Gaussianity [63].

$$\phi(B)(1 - B)^d y_t = c + \theta(B)\varepsilon_t + \boldsymbol{\beta}^\top \mathbf{x}_t \quad (5)$$

where:

y_t	is the dependent variable at time t ;
B	is the backshift operator, such that $By_t = y_{t-1}$;
$(1 - B)^d$	is the differencing operator applied d times;
$\phi(B)$	is the autoregressive (AR) polynomial;
c	is a constant;
$\theta(B)$	is the moving-average (MA) polynomial of order q , defined as $1 + \theta_1 B + \dots + \theta_q B^q$;
ε_t	is the white-noise innovation at time t (assumed i.i.d. with mean zero and finite variance);
$\mathbf{x}_t \in \mathbb{R}^k$	is a k -dimensional vector of exogenous covariates;
$\boldsymbol{\beta} \in \mathbb{R}^k$	is the vector of coefficients associated with the exogenous covariates;
$\boldsymbol{\beta}^\top \mathbf{x}_t$	represents the linear contribution of covariates to the forecast.

3.5 Time series foundation models

We benchmarked three pre-trained TSFM families in zero-shot modes with covariates. All models received the student enrolment history and, when applicable, a matrix of known covariates. Inputs were standardised using parameters computed on the training window and then inverted at the output.

3.5.1 Moirai

We applied Moirai, a TSFM family introduced by Salesforce, trained on large-scale multivariate time series spanning domains such as energy, transport, climate, cloud operations, and finance. The architecture was based on a masked-encoder transformer with any-variate attention. Multivariate inputs were supplied via `feat_dynamic_real_dim`, enabling targets and covariates to be represented jointly and partitioned into patches.

The Moirai-Small instantiated a 6-layer masked-encoder with model width $d_{\text{model}} = 384$, feed-forward width $d_{\text{ff}} = 1536$, and attention heads $n_{\text{heads}} = 6$, for approximately 14M parameters.

The Moirai-Base increased depth and width to 12 layers with $d_{\text{model}} = 768$, $d_{\text{ff}} = 3072$, and $n_{\text{heads}} = 12$, for roughly 91M parameters.

The Moirai-Large scaled to 24 layers with $d_{\text{model}} = 1024$, $d_{\text{ff}} = 4096$, and $n_{\text{heads}} = 16$, for about 311M parameters.

Moirai produced probabilistic forecasts by outputting parameters of a mixture distribution. Patch size was set to auto (from [8, 16, 32, 64, 128]), and inference settings included batch size and the number of samples drawn, with key and value dimension $d_{kv} = 64$ [18].

3.5.2 Chronos

We applied Chronos-Bolt and Chronos-2 as pre-trained time series foundation models that produced probabilistic multi-step forecasts. Chronos models were evaluated in their released capacity presets, and forecasts were generated without updating model weights. Where the implementation supported covariates, we supplied covariates through the model’s supported interface; otherwise, forecasts remained target-history conditioned. Chronos models were evaluated under consistent pre-processing and expanding-window evaluation, and produced quantile forecasts in a zero-shot setting. Chronos-Bolt can be combined with external covariate regressors, and Chronos-2 natively supports all covariate types [16, 50].

Chronos-Bolt-Tiny has approximately 9M parameters and is optimised for fast inference.

Chronos-Bolt-Mini has approximately 21M parameters and provides a balanced increase in representational capacity.

Chronos-Bolt-Small has approximately 48M parameters and offers greater expressive power for modelling non-linear temporal structure.

Chronos-Bolt-Base has approximately 205M parameters and enables rich temporal representations at the cost of higher computational demand.

Chronos-2 has approximately 120M parameters and serves as a general purpose time series foundation model with native support for covariates.

3.5.3 TimesFM

We applied TimesFM as a decoder-only pre-trained model designed to operate across variable context and horizon lengths. In the covariate setting, TimesFM generated a base forecast from the target history and then fitted a lightweight

linear model on the residuals using available covariates, yielding a covariate-aware forecast without modifying the core model weights.

The TimesFM-200M model has 200M parameters and 20 layers.

The TimesFM-500M model has 500M parameters and 50 layers.

The evaluated configurations used 16 attention heads, patch lengths (input/output) of 32/128, and an embedding dimension of 1280 [17].

3.6 Model evaluation

In student enrolment forecasting, error measures were used as the standard way to assess accuracy [64]. Mean Absolute Error (MAE) and Mean Squared Error / Root Mean Squared Error (MSE/RMSE) in Equations 6 and 7 were the most commonly reported metrics. MAE was especially interpretable, as it represented the average miss in the original units [65]. Both metrics compared a forecast \hat{y}_t with the observed enrolment y_t across T periods, but weighted errors differently, MAE averaged absolute errors, while RMSE averaged squared errors and then took the square root, placing additional emphasis on large misses [66].

$$\text{MAE} = \frac{1}{T} \sum_{t=1}^T |y_t - \hat{y}_t| \quad (6)$$

$$\begin{aligned} \text{MSE} &= \frac{1}{T} \sum_{t=1}^T (y_t - \hat{y}_t)^2, \\ \text{RMSE} &= \sqrt{\text{MSE}} = \sqrt{\frac{1}{T} \sum_{t=1}^T (y_t - \hat{y}_t)^2}. \end{aligned} \quad (7)$$

To enable cross-series comparison, the Symmetric Mean Absolute Percentage Error (SMAPE) in Equation 8 rescaled the absolute error by the average magnitude of the actual and forecast values. SMAPE was expressed as a percentage and bounded between 0% and 200%, but could be unstable when both y_t and \hat{y}_t were near zero [64].

$$\text{SMAPE} = \frac{100}{T} \sum_{t=1}^T \frac{2|y_t - \hat{y}_t|}{|y_t| + |\hat{y}_t|} \quad (8)$$

3.7 Evaluating probabilistic forecasts and calibration diagnostics

We evaluated probabilistic forecasts using proper (and ideally strictly proper) scoring rules. These loss functions aligned incentives by ensuring that the expected score was minimised only when the forecaster reported its true predictive distribution [67]. Building on the classical foundation for evaluating binary events, we relied on the broader theory of strictly proper rules applicable to both discrete and continuous outcomes [68]. This mathematical rigour was important because it ensured that improvements in metrics reflected genuine gains in predictive performance rather than artefacts of an arbitrary evaluation scheme [69].

For continuous targets, we used the Continuous Ranked Probability Score (CRPS), often reported alongside (and contrasted with) the logarithmic score [70]. CRPS evaluated global fit by comparing the entire predictive cumulative distribution function (CDF) in Equation 9, F , against the realised value, y :

$$\text{CRPS}(F, y) = \int_{-\infty}^{\infty} (F(z) - \mathbb{1}_{y \leq z})^2 dz \quad (9)$$

Beyond aggregate scores, we assessed distributional reliability via PIT. Under probabilistic calibration, realisations mapped through the predicted CDF should behave as uniform noise and follow a Uniform distribution $\mathcal{U}[0, 1]$ [71]. PIT diagnostics were used to visually detect bias, overconfidence, and under-dispersion, following established practice in econometrics and meteorology [72]. In addition to significance testing, we reported effect sizes to quantify the *magnitude* of improvement in a way that remained interpretable under data sparsity. For point accuracy, we computed paired differences relative to a reference baseline.

3.8 Experiment setup

We implemented a reproducible forecasting pipeline with strict vintage control (Figure 2). Processing operated at the yearly level; we aligned all series to a common year index and standardised features within each training window to prevent information leakage. Model evaluation followed an expanding-window backtest for each annual forecast origin.

3.8.1 Task definition

We studied annual year-ahead forecasting of new enrolments in a higher-education institutional planning setting. New enrolments referred to students commencing their studies at the institution in the given academic year. The target series was observed at an annual cadence and was disaggregated into institutional cohorts. The annual sampling and short history imposed severe data sparsity, motivating the use of zero-shot TSFMs and an external covariate.

3.8.2 Backtesting protocol

We adopted an expanding-window backtest. At each forecast origin year t , models produced a one-year-ahead forecast for $t+1$ using only information that would have been available at time t . All external covariates were lagged and vintage-aligned to the forecast origin to avoid leakage. This protocol was designed to reflect a decision-time institutional workflow: forecasts were generated annually for planning, and covariate availability was constrained by publication timing and platform release schedules.

3.8.3 Models and baselines

We benchmarked multiple TSFMs in a strict zero-shot configuration. We compared against a reference baseline suitable for annual planning. For TSFMs that output predictive distributions, we evaluated both point and probabilistic quality. Model variants were treated as a controlled factor to assess whether covariate conditioning interacted with model capacity under sparsity.

3.8.4 Covariate sets and ablation design

External information was introduced via a compact, leakage-safe covariate set with explicit availability rules. We structured the experiment as an ablation grid over covariate regimes. This design clarified, under annual sparsity, when leakage-safe covariates improved zero-shot TSFMs and when they introduced brittle conditioning behaviours.

3.8.5 Evaluation metrics and diagnostics

We reported both point and probabilistic forecast performance. For point accuracy, we used error metrics, supplemented with scale-normalised error measures where appropriate to support comparisons across cohorts and periods. To summarise practical magnitude, we reported paired differences and effect sizes relative to a reference baseline, quantifying the size of improvements in a way that remained interpretable under short, annual histories.

3.8.6 Reporting and reproducibility

To support auditability, we reported covariate availability rules, lag choices, and feature-engineering steps alongside the backtesting configuration. Where data was restricted, we specified an explicit data-availability statement and provided sufficient procedural detail to allow reproduction of the evaluation and covariate construction steps on other institutions' data.

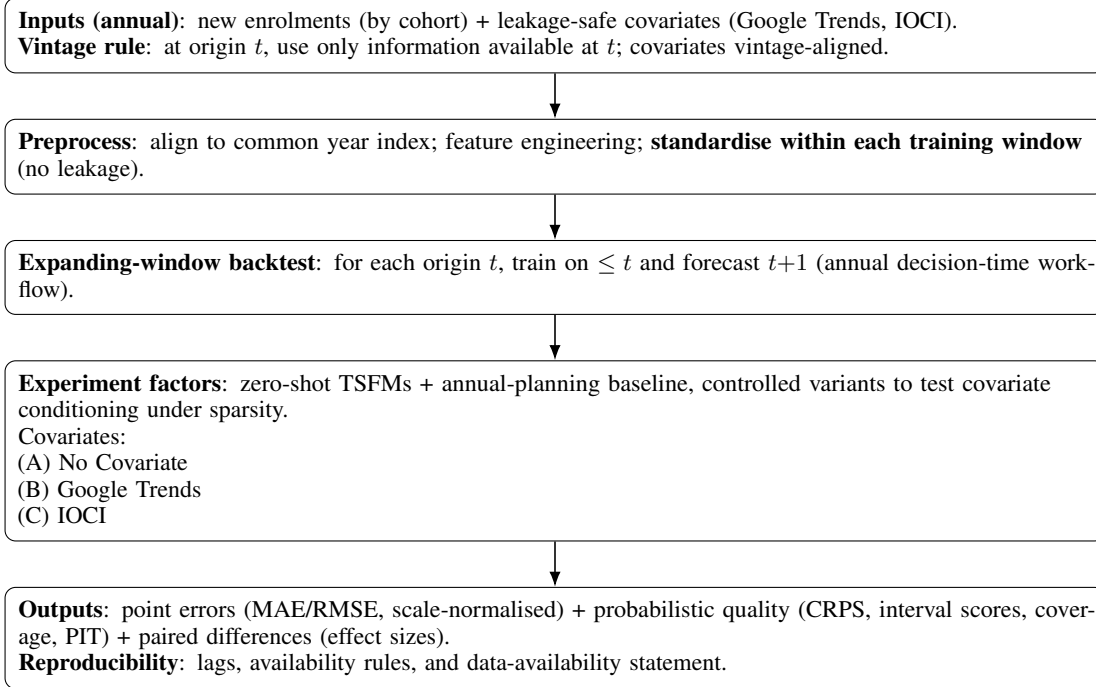


Figure 2: Experiment workflow.

4 Experimental results and analysis

This section reports forecasting accuracy across model classes under input settings. We summarise performance using error metrics.

4.1 Forecast Analysis of Model Evaluation Results

Table 2 summarises per-cohort, per-condition rankings by ordering models within each covariate setting on the four error measures (MAE, RMSE, SMAPE, MAPE), then averaging ranks across metrics and horizons. This shows an interpretable score per model for each cohort that reflects performance.

4.1.1 Domestic cohort

In Figure 3 for new domestic enrolments, adding calibrated IOCI substantially improves the Chronos-Bolt family, with consistent gains in error metrics. This change reorders the relative performance ranking in favour of Chronos variants. By contrast, Persistence drops in rank, while TimesFM and ARIMA degrade substantially when the IOCI covariate is introduced. These results suggest that calibrated IOCI is most beneficial when the models can exploit it.

4.1.2 International cohort

In Figure 4 for new international enrolments, the no-covariate setting is led by Moirai-Small, which attains the lowest errors and ranks first overall. Introducing engineered Google Trends features does not produce uniform gains within the Trends-augmented setting. Moirai-Base becomes the top-ranked model, followed closely by Moirai-Small, while the strongest Chronos variant under Trends is Chronos-Bolt-Base. This pattern indicates that Trends behaves as a selective demand-proxy signal helpful for some model families, improving Moirai-Base and Chronos-Bolt-Base, but degrading others notably Moirai-Small, relative to its no-covariate performance.

Table 2: Model comparisons metrics all results for domestic and international students enrolment (good = green, orange = moderate, red = bad).

Covariates	Model	MAE	RMSE	SMAPE	MAPE	MAE Rank
Domestic student						
No Covariate	Chronos-Bolt-Tiny	358.1	455.3	6.1	6.3	1
	Persistence	371.5	456.6	6.4	6.7	2
	Chronos-Bolt-Small	372.6	480.3	6.3	6.5	3
	Chronos-Bolt-Mini	376.5	461.5	6.4	6.7	4
	Chronos-2	386.3	481.9	6.6	6.9	5
	TimesFM-500	395.7	479.9	6.8	7.1	6
	TimesFM-200	397.3	511.0	6.8	7.2	7
	Chronos-Bolt-Base	406.7	491.8	7.0	7.3	8
	Morai-Small	506.2	621.6	8.6	9.1	9
	ARIMA	508.8	614.9	8.4	8.9	10
IOCI	Morai-Large	519.5	626.4	8.8	9.3	11
	Morai-Base	531.5	656.8	9.1	9.6	12
	Chronos-Bolt-Tiny	321.3	431.9	5.5	5.8	1
	Chronos-Bolt-Small	324.0	423.6	5.5	5.8	2
Chronos-2	Chronos-Bolt-Base	347.0	438.3	6.0	6.3	3
	Chronos-Bolt-Mini	348.5	431.2	6.0	6.3	4
	Persistence	371.5	456.6	6.4	6.7	5
	Chronos-2	387.7	504.7	6.6	7.0	6
	Morai-Small	496.6	611.0	8.4	9.0	7
	TimesFM-500	509.8	583.3	9.0	9.4	8
	Morai-Base	528.5	662.9	9.0	9.7	9
	TimesFM-200	532.4	618.2	9.4	9.9	10
	Morai-Large	628.9	843.3	10.3	11.3	11
	ARIMA	698.1	786.1	12.1	13.0	12
International student						
No Covariate	Morai-Small	168.8	180.9	14.7	15.0	1
	Morai-Base	183.6	197.5	16.9	17.0	2
	Chronos-Bolt-Small	189.3	200.2	17.8	18.0	3
	Chronos-Bolt-Mini	200.5	218.8	19.0	18.7	4
	Chronos-2	201.0	210.0	18.3	18.8	5
	Chronos-Bolt-Tiny	205.2	216.4	19.1	19.6	6
	Chronos-Bolt-Base	208.9	222.7	19.4	19.1	7
	Persistence	209.6	225.5	19.2	20.0	8
	ARIMA	217.8	234.3	19.2	19.9	9
	Morai-Large	222.4	231.0	20.0	20.5	10
Google Trends	TimesFM-500	226.6	248.3	20.8	20.7	11
	TimesFM-200	236.4	258.0	21.2	21.3	12
	Morai-Base	181.3	190.0	16.6	17.6	1
	Morai-Small	181.7	192.6	15.7	16.4	2
Chronos-2	Chronos-Bolt-Base	190.8	215.6	17.8	17.4	3
	Chronos-Bolt-Mini	196.4	215.4	18.0	18.2	4
	Chronos-Bolt-Small	202.6	225.1	18.9	19.1	5
	Persistence	209.6	225.5	19.2	20.0	6
	Chronos-2	212.1	228.7	19.3	19.7	7
	Chronos-Bolt-Tiny	212.3	235.4	20.7	20.3	8
	Morai-Large	230.3	241.8	20.9	21.3	9
	TimesFM-200	232.6	269.4	21.0	21.3	10
	TimesFM-500	238.6	273.0	21.6	22.2	11
	ARIMA	364.1	424.3	33.8	38.2	12

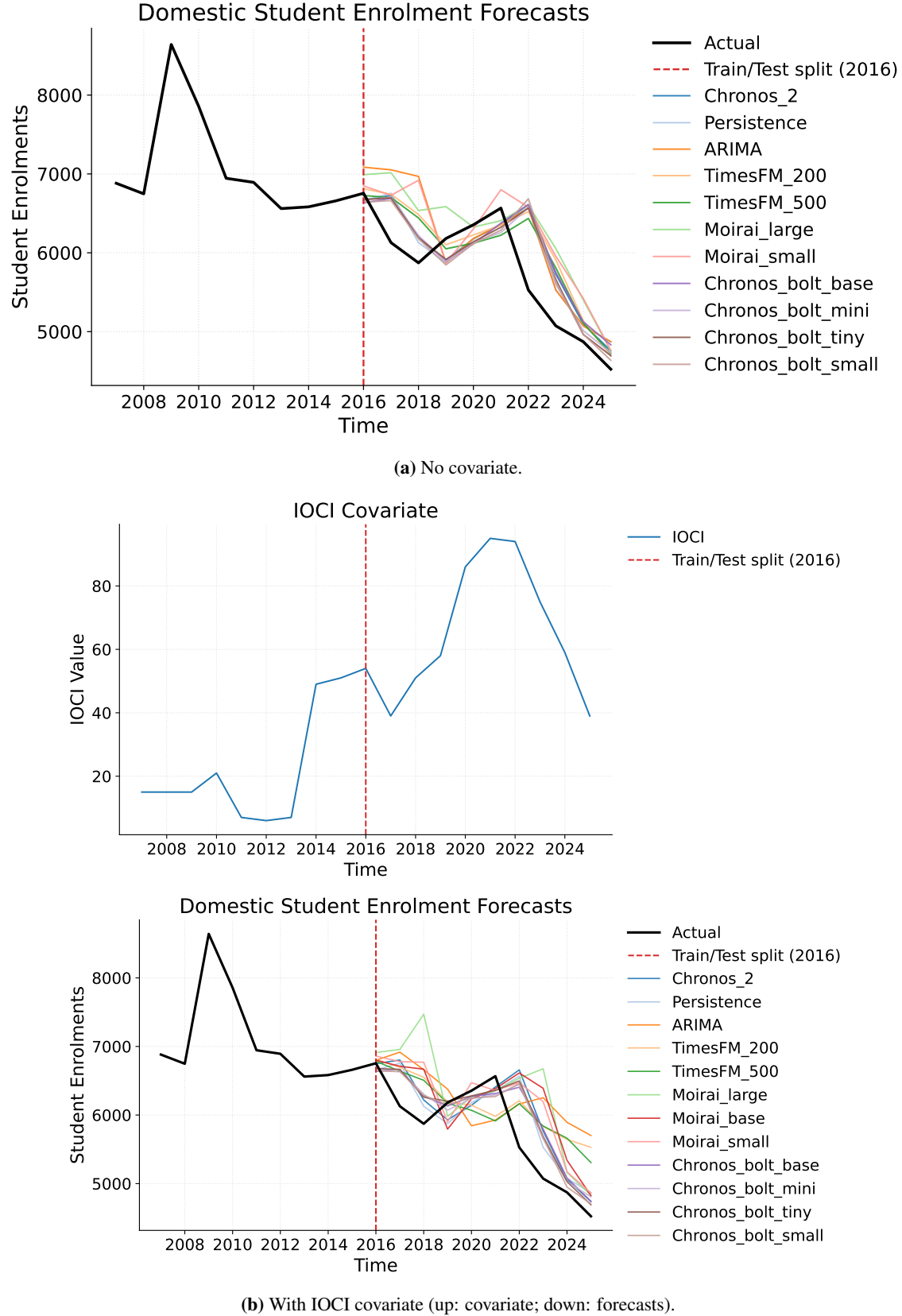


Figure 3: Actuals and forecasts of annual new domestic-student enrolments. Panel (a) shows unconditional forecasts. Panel (b) shows IOCI covariate and covariate-conditioned forecasts. The red dashed line marks the forecast origin year.

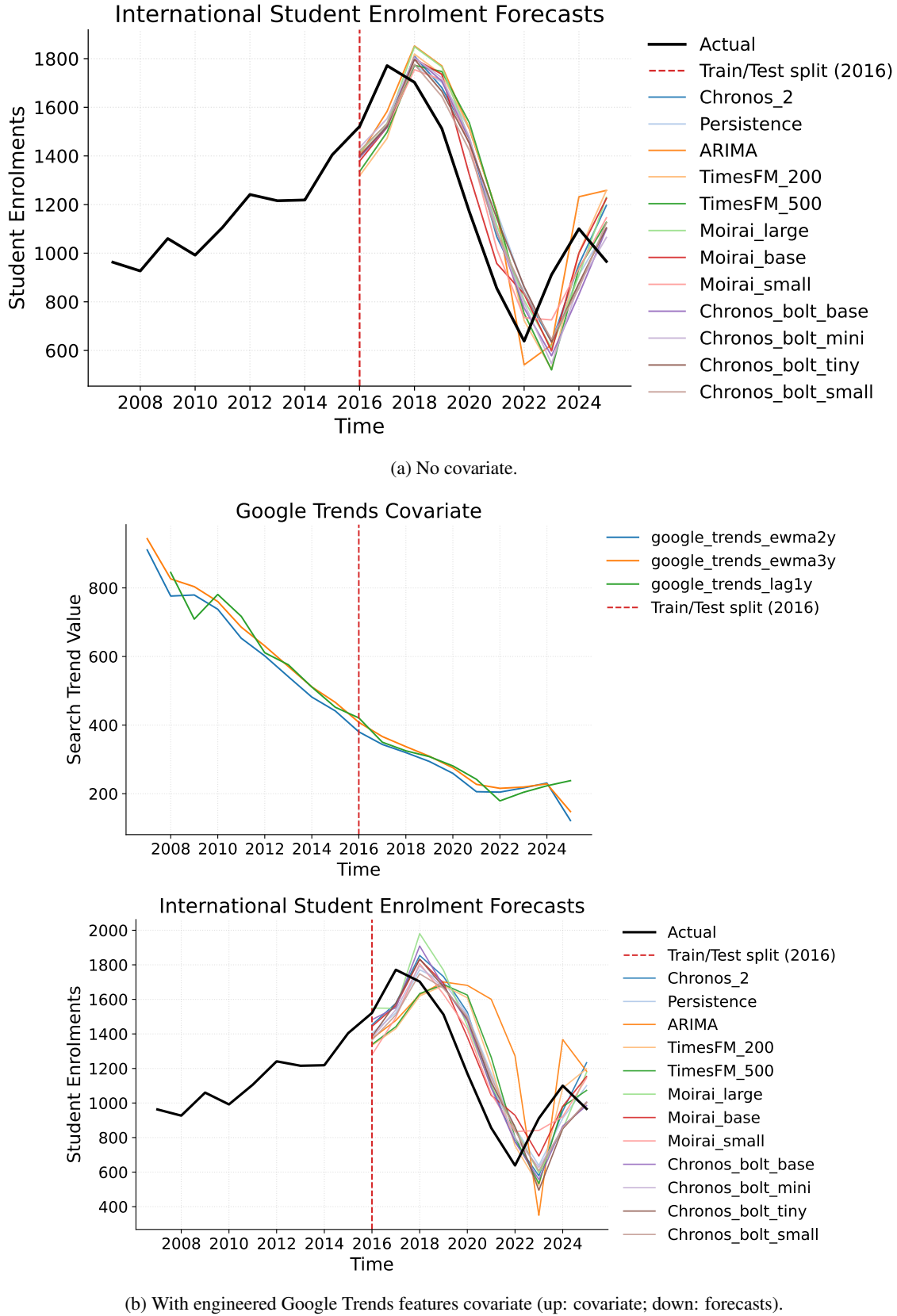


Figure 4: Actuals and forecasts of annual new international-student enrolments. Panel (a) shows unconditional forecasts. Panel (b) shows engineered Google Trends features covariate and covariate-conditioned forecasts. The red dashed line marks the forecast origin year.

4.1.3 Effect of covariates

The results indicate a clear covariate interaction, where engineered features derived from Google Trends and IOCI improve accuracy for several models. For domestic enrolments, IOCI acts as a stabilising covariate for the Chronos-Bolt family, delivering consistent improvements and preserving Chronos-Bolt-Tiny as the best model. However, ARIMA and TimesFM do not benefit from this covariate and degrade when IOCI is introduced, suggesting limited capacity to exploit the signal without amplifying variance.

For international enrolments, the impact of Google Trends is mixed. Under Trends conditioning, Moirai-Base ranks first, and Chronos-Bolt-Base and Chronos-Bolt-Mini improve relative to their no-covariate counterparts. Operationally, this suggests that Trends features should be treated as an optional covariate: they can improve performance for some model families but are not uniformly beneficial.

4.1.4 Effect Size and Probabilistic Calibration

Table 3: Effect Size and CRPS Summary

Cohort	Covariates	Model	ΔMAE	CRPS (80%)	CRPS (95%)
Domestic	None	Chronos-Bolt-Tiny	13.5	254.7	284.4
Domestic	IOCI	Chronos-Bolt-Tiny	50.22	239.7	269.5
Domestic	IOCI	Chronos-Bolt-Small	47.49	243.9	275.1
Domestic	IOCI	Chronos-Bolt-Mini	23.04	249.5	281.2
Domestic	IOCI	Chronos-Bolt-Base	24.47	256.7	293.3
International	None	Moirai-Small	40.8	105.4	113.1
International	None	Moirai-Base	26.0	117.7	129.3
International	None	Chronos-Bolt-Small	20.3	120.1	129.8
International	None	Chronos-Bolt-Mini	9.1	127.9	138.8
International	None	Chronos-2	8.6	127.7	138.9
International	None	Chronos-Bolt-Tiny	4.4	130.6	143.2
International	None	Chronos-Bolt-Base	0.7	135.9	149.6
International	Google Trends	Moirai-Base	28.3	119.1	129.6
International	Google Trends	Moirai-Small	27.9	119.9	130.5
International	Google Trends	Chronos-Bolt-Base	18.8	135.7	154.1
International	Google Trends	Chronos-Bolt-Mini	13.3	131.1	145.8
International	Google Trends	Chronos-Bolt-Small	7.0	144.6	166.8

Table 3 provides a compact summary of both practical accuracy gains and probabilistic forecast quality across cohorts, covariate settings, and time series foundation models. The table is organised by cohort, then by the type of external information available to the model, and finally by the specific forecasting model configuration. For each row, $\Delta\text{MAE} = \text{MAE}_{\text{Persistence}} - \text{MAE}_{\text{Model}}$, summarising the magnitude of point-error relative to the reference baseline and an effect size indicator of improvement. Furthermore, CRPS 80% and CRPS 95% summarise probabilistic performance at the 80% and 95% levels, where lower values indicate better uncertainty-aware forecasts. In our setting, several forecasters provide discrete predictive quantiles rather than full parametric densities or large ensembles of samples, so we compute CRPS using a quantile-based approximation. CRPS (80%) is computed from the quantiles of the central 80%, while CRPS (95%) is computed from the quantiles of the central 95%. These interval scores capture miscalibration penalties in a single proper metric, and provide a distribution-level complement to point errors under annual data sparsity. Overall, these results support an interpretation of contribution as directional and configuration-dependent: covariates such as IOCI and Google Trends can improve both point and probabilistic performance, but the magnitude and consistency of those improvements depend on the cohort, the model family, and the stability of covariate conditioning under small-sample backtesting.

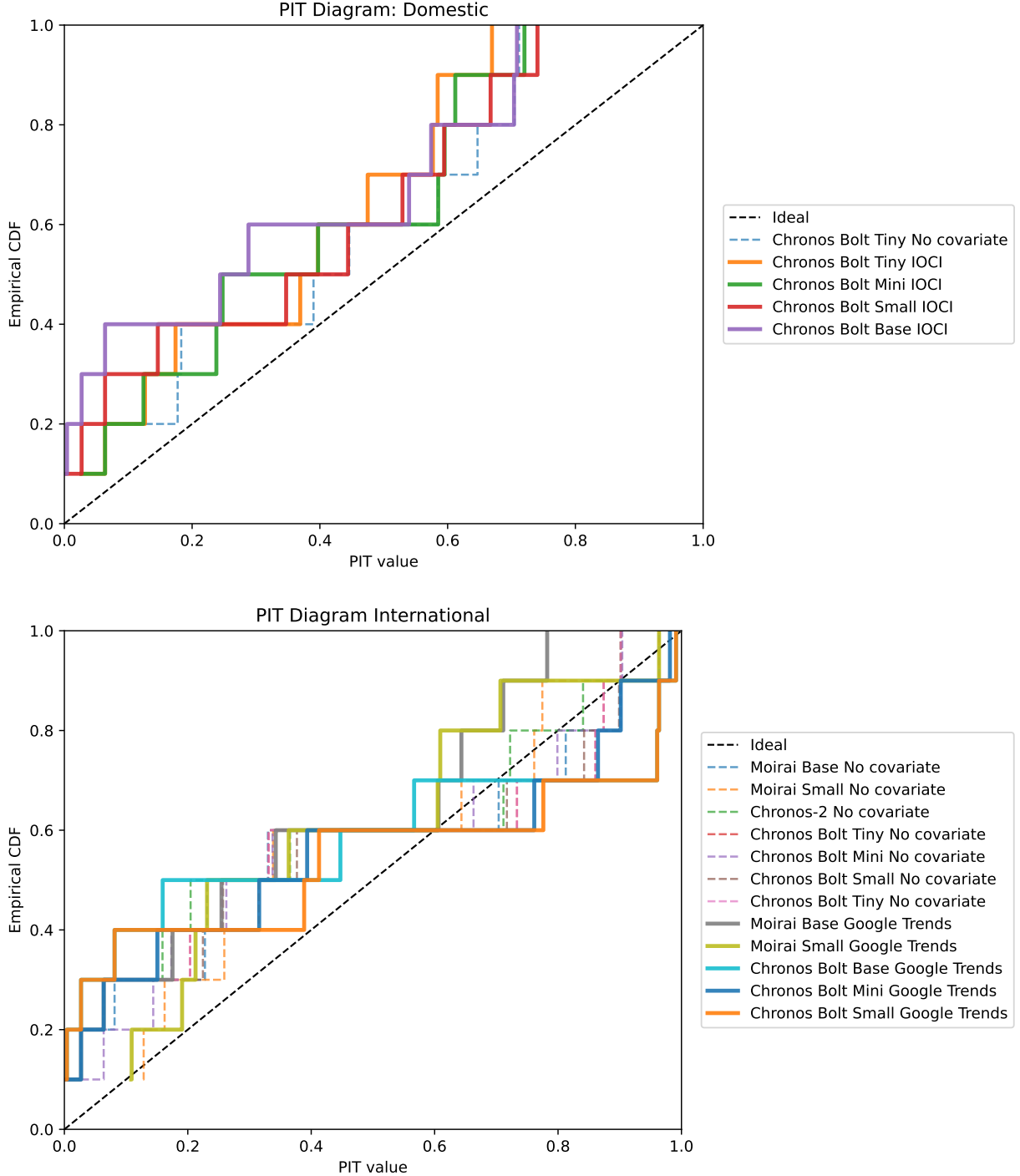


Figure 5: CDF of probability integral transform

Figure 5 reports the empirical CDF of Probability Integral Transform (PIT) values, a standard diagnostic for distributional calibration. For each forecast origin t , the PIT value is $u_t = F_t(y_t)$, the predictive CDF evaluated at the realised outcome is under ideal calibration $u_t \sim \text{Uniform}(0, 1)$ and the empirical CDF of $\{u_t\}$ follows the 45° reference line.

In the domestic cohort, the no-covariate is compared with IOCI-conditioned Chronos-Bolt variants. The IOCI-conditioned curves lie closer to the diagonal across much of the PIT range, indicating improved probabilistic calibration.

While departures from the reference remain, the overall shift towards the diagonal is consistent with IOCI providing additional regime information that improves the alignment between predictive distributions and realised outcomes.

In the international cohort, Google Trends configurations generally track the reference line more closely than their no-covariate counterparts, particularly through the middle-to-upper PIT range. This pattern is consistent with features improving the allocation of probability mass in periods of strong demand variation. However, several model-covariate combinations still exhibit pronounced deviations, underscoring that calibration gains are configuration-dependent rather than universal.

4.2 Forecast analysis of new domestic student enrolment

The domestic tertiary sector exhibits gradual year-to-year aggregate movements. This inherent stability renders simple extrapolative benchmarks surprisingly competitive, particularly given the modest domestic growth observed in the recent sector. In this analysis, we evaluate domestic new enrolment forecasts using an expanding window backtesting design, comparing classical baselines against zero-shot TSFMs under varying covariate specifications.

Time series for new domestic enrolments is characterised by a relatively smooth medium-run evolution. Consistent with this hypothesis, the naive Persistence baseline serves as a rigorous benchmark. Among the TSFMs, the compact Chronos-Bolt variants demonstrate superior performance, suggesting they effectively regularise within limited historical windows. In the absence of external covariates, Chronos-Bolt-Tiny is followed closely by the Persistence baseline and Chronos-Bolt-Small. The remaining Chronos and TimesFM variants occupy an intermediate position, whereas Moirai variants and ARIMA exhibit higher errors.

Incorporation of IOCI reveals a heterogeneous response. The Chronos-Bolt family derives substantial benefit from this covariate: Chronos-Bolt-Tiny and Chronos-Bolt-Small improved under IOCI, representing ΔMAE of 50.22 and 47.49 relative to Persistence, respectively. Conversely, TimesFM and ARIMA performance degrade sharply upon the introduction of the index. This divergence suggests that while IOCI contains a stabilising regime-aware signal, utility is contingent on the model's conditioning mechanism. The additional covariate channel can amplify misspecification and induce brittle extrapolation. In the expanding-window backtests, IOCI improved domestic forecasts for specific TSFM configurations but did not improve international forecasts consistently; we therefore retained IOCI only in settings where it provided an incremental signal.

Across the evaluated configurations, Chronos-Bolt-Tiny provides the most favourable accuracy-stability trade-off under the no-covariate setting. When a leakage-safe institutional context signal is available, conditioning Chronos-Bolt-Tiny and, in some settings, Chronos-Bolt-Small on IOCI confers additional reductions in error. Chronos-Bolt-Tiny has stable performance. When a leakage-safe institutional context signal is available, Chronos-Bolt-Tiny and Chronos-Bolt-Small conditioned on IOCI are recommended for improved accuracy and more regime-aware tracking. Classical models with covariates (ARIMAX) require careful diagnostics and can degrade materially under short samples and structural change. The reductions in point errors for the Chronos variants are consistent with what we expect under annual sampling and short evaluation windows against the Persistence baseline.

4.3 Forecast analysis of new international student enrolment

New international student enrolments exhibit heightened sensitivity to exogenous shocks, with abrupt deviations driven by border settings, visa policy, geopolitical risk, and shifts in perceived destination attractiveness. Consistent with this macro-sensitivity, international commencing enrolments rebounded in 2024 relative to 2023, although they remained below pre-pandemic levels, underscoring ongoing structural uncertainty.

The international time series displays greater variance and more pronounced turning-point behaviour. Consequently, purely autoregressive baselines risk lagging during rapid upswings or drawdowns. In such settings, model efficacy is often enhanced by architectures with strong cross-domain priors, such as TSFMs and the inclusion of leakage-safe external proxies that capture demand intent. However, the utility of exogenous signals depends on the downstream model family and the stability of the covariate transformations.

In the univariate setting, excluding covariates, Moirai-Small demonstrates superior accuracy, followed by Moirai-Base and Chronos-Bolt Small. While classical baselines remain competitive, TimesFM variants and ARIMA trail the top-performing TSFMs. This performance hierarchy suggests that for international demand, masked-encoder TSFMs (Moirai) provide a strong default prior even in the absence of explicit exogenous inputs, plausibly reflecting the ability to generalise multiscale structure learned during pre-training.

The engineered Google Trends features induce a material shift in the performance hierarchy. Moirai-Base ascends to the top rank. Conversely, Moirai-Small cedes its lead. The divergence in response is informative. While Chronos variants

can leverage the Trends signal, ARIMA performance deteriorates, indicating sensitivity to covariate misspecification and instability under short samples.

These results suggest Google Trends acts as a selective demand-proxy signal, the benefit of which is contingent on the structural compatibility between the covariate conditioning and the forecasting model. Despite these gains for the best-performing models, improvements are configuration-dependent and should be interpreted cautiously given annual sampling and the limited number of forecast origins.

5 Discussion

5.1 TSFMs zero-shot effectiveness in student new enrolment forecasting

For **RQ1**, state-of-the-art TSFMs demonstrate strong effectiveness for zero-shot forecasting of new student enrolments, particularly in institutional settings characterised by limited historical data, privacy constraints, and exposure to external shocks. Across domestic and international enrolment cohorts, zero-shot TSFMs consistently match or outperform classical benchmarks without requiring task-specific fine-tuning. Empirically, models equipped with appropriate inductive biases exhibit robust generalisation under data sparsity. Compact models, such as Chronos-Bolt-Tiny and Chronos-Bolt-Small, perform especially well for domestic enrolments, where the data-generating process is relatively smooth and dominated by short-to-medium memory.

Pre-trained models' priors provide effective regularisation, enabling stable forecasts that exceed baselines. Larger TSFM variants do not necessarily yield superior performance in this regime, highlighting that increased capacity can amplify noise when sample sizes are small.

For new international enrolments, which are more sensitive to exogenous shocks, masked-encoder TSFMs such as Moirai-Small and Moirai-Base achieve the strongest zero-shot accuracy in the absence of covariates. This suggests that broad cross-domain pre-training enables these models to internalise generic patterns associated with regime shifts and recovery dynamics. When leakage-safe external covariates are introduced, particularly engineered Google Trends features, Moirai-Base becomes the top-performing model, indicating that masked-encoder TSFMs can exploit demand-proxy signals when conditioning is stable.

These gains are achieved without institutional fine-tuning and reducing deployment overhead with the small number of annual forecast origins. Nonetheless, the consistent reductions in point-error metrics across cohorts and covariate settings indicate clear practical value. The results support TSFMs as a scalable, low-maintenance, and competitive solution for student enrolment forecasting, with performance contingent on model capacity, cohort characteristics, and the availability of well-designed exogenous signals.

5.2 Effectiveness of limited and sparse data TSFMs in zero-shot with covariate forecasting

For **RQ2**, covariate-conditioned TSFMs remained effective under limited and sparse institutional data provided that covariates were leakage-safe and aligned to the forecast origin, the covariate signal was sufficiently smooth and informative at annual frequency, and the model architecture incorporated exogenous channels without destabilising extrapolation. In short samples, models benefit from strong pre-trained priors that act as implicit regularisation; however, the incremental value of covariates is heterogeneous and model dependent.

In the domestic cohort, where annual new enrolments evolve relatively smoothly, smaller Chronos-Bolt variants remain robust and improve further when conditioned on IOCI. Even with sparse annual histories, a compact TSFM can exploit a stable, regime-aware covariate to reduce error. This is consistent with the view that covariates can provide a low-dimensional summary of exogenous conditions that a short target history cannot fully encode.

In the international cohort, which exhibits stronger non-stationarity and shock sensitivity, Moirai variants provide strong zero-shot performance even without covariates, suggesting that masked encoders carry a useful cross-domain prior for volatile demand series. When engineered Google Trends covariates are added, Moirai-Base becomes the top performer. This pattern supports the claim that, under sparsity, covariates can materially improve forecasts when they function as demand-intent proxies and when the model family can condition on them stably.

However, sparsity also amplifies the risk of brittle covariate use. Classical ARIMAX and some TSFM configurations degrade when covariates are introduced, illustrating that exogenous inputs can induce misspecification when the sample is short and turning points dominate. For example, in the domestic cohort, TimesFM and ARIMA worsen substantially under the IOCI covariate. Similarly, in the international cohort, ARIMA deteriorates sharply under Google Trends. These outcomes underline that covariate integration is not uniformly beneficial and requires careful design and diagnostics in annual settings with few forecast origins. Practically, the evidence supports the conclusion that

covariate-conditioned models remain operationally strong under limited data, but the advantage is best interpreted as a robust, repeatable reduction in forecast error rather than a universal improvement under classical testing.

5.3 Select effective covariates and feature engineered to improve TSFMs performance

For **RQ3**, selective covariates and feature engineering improve student enrolment forecasting by injecting structured, low-dimensional information about exogenous drivers that cannot be reliably inferred from short and sparse target histories alone. In data-scarce institutional settings, the target series provides limited evidence about regime shifts, demand shocks, and structural constraints; well-designed covariates therefore act as stabilising contextual signals that complement the pre-trained temporal priors of TSFMs.

First, selective covariates summarise external conditions that directly influence enrolment dynamics. Demand-proxy variables, such as engineered Google Trends features, while institutional context measures such as IOCI, capture regime-level stress associated with settings, and organisational restructuring. When covariates are leakage-safe, temporally aligned, and available at the forecast origin, they provide information that is orthogonal to autoregressive history, enabling models to adjust level and trajectory forecasts more rapidly around turning points.

Second, feature engineering is critical for transforming noisy raw signals into forms that are usable under sparsity. Simple lagged features inject short-run persistence without violating causality, while exponentially weighted moving averages (EWMA) suppress high-frequency noise and emphasise medium-run trends that are more compatible with annual decision horizons. These transformations improve signal-to-noise ratios and reduce variance, allowing the architecture to condition on covariates without overreacting to transient fluctuations. Empirically, engineered covariates consistently outperform raw covariate inputs, particularly for volatile international enrolment series where unprocessed signals can induce instability.

Third, covariate effectiveness depends on interaction with model architecture. Models with explicit and stable covariate-conditioning mechanisms, such as Chronos-Bolt, can exploit engineered features to deliver meaningful accuracy gains under limited data. In contrast, models with weaker or more rigid exogenous handling, including classical ARIMAX and some decoder-only configurations, can degrade when covariates are introduced, showing that feature engineering alone is insufficient without architectural compatibility. This interaction effect explains why covariates improve performance selectively rather than universally across models.

Therefore, selective covariates and feature engineering enhance predictive robustness, not only average accuracy. Under regime shifts, covariate-conditioned models track directional changes more consistently than purely autoregressive baselines. Although formal tests have limited power in short annual samples, the repeated reductions in point-error metrics across cohorts and forecast origins indicate that covariates and feature engineering yield operationally meaningful improvements.

5.4 Limitations and future work

Despite encouraging results, this study has several limitations that motivate clear directions for future research. The primary limitation is the annual frequency and short historical length of institutional enrolment data. While this reflects real-world constraints faced by universities, it reduces the statistical power of model-comparison tests and limits the ability to detect small but systematic differences in forecasting accuracy.

Future work should evaluate a broader range of leakage-safe covariates, including demographic projections, labour-market indicators, timestamped events, and text-derived signals from news and institutional communications. It should also extend the analysis to higher-frequency settings where available, enabling richer temporal structure, stronger inferential power, and more granular decision support. Although the study shows that carefully engineered covariates can materially improve zero-shot TSFM performance, the covariate set is intentionally compact and cannot fully capture heterogeneous drivers such as programme-level demand, scholarship availability, and behavioural responses.

6 Conclusion

This study evaluates the efficacy of state-of-the-art TSFMs in forecasting student enrolments under challenging institutional conditions characterised by short histories, privacy constraints, and external volatility. Through a systematic zero-shot evaluation of domestic and international cohorts, we compared leading TSFMs against classical baselines and assessed the impact of engineered, leakage-safe covariates. Zero-shot TSFMs consistently outperform traditional methods in data-sparse environments without requiring site-specific fine-tuning. Compact models such as Chronos-Bolt capture the relatively stable dynamics of domestic enrolment well, while masked-encoder architectures such as Moirai appear more resilient under the higher volatility observed in international enrolment series. Exogenous variables

particularly engineered Google Trends features, and IOCI yield additional accuracy gains when they are temporally aligned, low-dimensional, and paired with architectures that support stable covariate conditioning. Conversely, several classical models and some configurations degrade when covariates are introduced, underscoring that exogenous information is not universally beneficial under sparsity and must be integrated with appropriate diagnostics.

References

- [1] I-Hong Kuo, Shi-Jinn Horng, Tzong-Wann Kao, Tsung-Lieh Lin, Cheng-Ling Lee, and Yi Pan. An improved method for forecasting enrollments based on fuzzy time series and particle swarm optimization. *Expert Systems with Applications*, 36(3, Part 2):6108–6117, 2009. ISSN 0957-4174. doi:10.1016/j.eswa.2008.07.043. URL <https://www.sciencedirect.com/science/article/pii/S0957417408004818>.
- [2] Yao-Lin Huang, Shi-Jinn Horng, Mingxing He, Pingzhi Fan, Tzong-Wann Kao, Muhammad Khurram Khan, Jui-Lin Lai, and I-Hong Kuo. A hybrid forecasting model for enrollments based on aggregated fuzzy time series and particle swarm optimization. *Expert Systems with Applications*, 38(7):8014–8023, 2011. ISSN 0957-4174. doi:10.1016/j.eswa.2010.12.127. URL <https://www.sciencedirect.com/science/article/pii/S0957417410014909>.
- [3] Robert Kelchen and Holly Evans. Examining the relationship between institutional financial stress and student enrollment. Working Paper 24-05, Federal Reserve Bank of Philadelphia, July 2024. URL https://robertkelchen.com/wp-content/uploads/2024/07/hcm_enrollment_jul24.pdf. Verified [web:22][web:27][page:0].
- [4] Nathan D Grawe. *Demographics and the Demand for Higher Education*. Johns Hopkins University Press, Baltimore, MD, 2018. Verified [web:21][web:26].
- [5] Kelli A Bird. Predictive analytics in higher education: The promises and challenges of using machine learning to improve student success. *AIR Professional File*, (161):1–18, 2023. URL https://www.airweb.org/docs/default-source/aha/apf-161-predictive-analytics-in-higher-education.pdf?sfvrsn=f31dcce4_1. Fall 2023, Article 161. Verified [web:23][page:1].
- [6] K Willis and P Yang. Towards redefining strategic enrollment management: Response to emerging challenges of the 21st century. *Journal of Advancing Education Practice*, 5(2):45–58, 2024. URL <https://openriver.winona.edu/jaep/vol5/iss2/7/>. Verified, vol.5 iss.2 [web:24].
- [7] J M Mendez et al. Analyzing and forecasting enrolment patterns using time series models. *International Journal of Advanced Computer Science*, 12(1):102–115, 2025. Unverified exact match; related works exist [web:25][web:30].
- [8] Organisation for Economic Co-operation and Development. The financial sustainability of higher education: Insights from policy in oecd countries, 2025. URL https://www.oecd.org/en/publications/the-financial-sustainability-of-higher-education_f544ccfe-en.html. Published 24 November 2025 [web:9].
- [9] Organisation for Economic Co-operation and Development. Education at a glance 2024: Oecd indicators, 2024. URL https://www.oecd-ilibrary.org/education/education-at-a-glance-2024_c00cad36-en. Published 10 September 2024 [web:2][web:10].
- [10] Bridget Terry Long. *The Financial Crisis and College Enrollment: How Have Students and Their Families Responded?*, pages 209–233. University of Chicago Press, January 2014. doi:10.7208/chicago/9780226201979.003.0007. URL <http://www.nber.org/chapters/c12862>.
- [11] Elliot N. Maltz, Kenneth E. Murphy, and Michael L. Hand. Decision support for university enrollment management: Implementation and experience. *Decision Support Systems*, 44(1):106–123, 2007. ISSN 0167-9236. doi:10.1016/j.dss.2007.03.008. URL <https://www.sciencedirect.com/science/article/pii/S016792360700053X>.
- [12] Xinshuai Li, Senlin Luo, Limin Pan, and Zhouting Wu. Adapt to small-scale and long-term time series forecasting with enhanced multidimensional correlation. *Expert Systems with Applications*, 238:122203, 2024. ISSN 0957-4174. doi:10.1016/j.eswa.2023.122203. URL <https://www.sciencedirect.com/science/article/pii/S0957417423027057>.
- [13] Spyros Makridakis, Evangelos Spiliotis, and Vassilios Assimakopoulos. The m4 competition: 100,000 time series and 61 forecasting methods. *International Journal of Forecasting*, 36(1):54–74, 2020. ISSN 0169-2070. doi:10.1016/j.ijforecast.2019.04.014. URL <https://www.sciencedirect.com/science/article/pii/S0169207019301128>. M4 Competition.

[14] Christoph Bergmeir, Rob J. Hyndman, and Bonsoo Koo. A note on the validity of cross-validation for evaluating autoregressive time series prediction. *Computational Statistics & Data Analysis*, 120:70–83, 2018. ISSN 0167-9473. doi:10.1016/j.csda.2017.11.003. URL <https://www.sciencedirect.com/science/article/pii/S0167947317302384>.

[15] Daniel Bolaños-Martinez, Alberto Durán-López, Jose Luis Garrido, Blanca Delgado-Márquez, and María Bermudez-Edo. Sasd: Self-attention for small datasets—a case study in smart villages. *Expert Systems with Applications*, 271:126245, 2025. ISSN 0957-4174. doi:10.1016/j.eswa.2024.126245. URL <https://www.sciencedirect.com/science/article/pii/S0957417424031129>.

[16] Abdul Fatir Ansari, Lorenzo Stella, Caner Turkmen, Xiyuan Zhang, Pedro Mercado, Huibin Shen, Oleksandr Shchur, Syama Syndar Rangapuram, Sebastian Pineda Arango, Shubham Kapoor, Jasper Zschiegner, Danielle C. Maddix, Michael W. Mahoney, Kari Torkkola, Andrew Gordon Wilson, Michael Bohlke-Schneider, and Yuyang Wang. Chronos: Learning the language of time series. *Transactions on Machine Learning Research*, 2024. ISSN 2835-8856. URL <https://openreview.net/forum?id=gerNCVqqtR>.

[17] Abhimanyu Das, Weihao Kong, Rajat Sen, and Yichen Zhou. A decoder-only foundation model for time-series forecasting, 2024. URL <https://arxiv.org/abs/2310.10688>.

[18] Gerald Woo, Chenghao Liu, Akshat Kumar, Caiming Xiong, Silvio Savarese, and Doyen Sahoo. Unified training of universal time series forecasting transformers. In *Forty-first International Conference on Machine Learning*, 2024.

[19] ZhuoLin Li, ZiHeng Gao, XiaoLin Zhang, GaoWei Zhang, and LingYu Xu. Time-aware personalized graph convolutional network for multivariate time series forecasting. *Expert Systems with Applications*, 240:122471, 2024. ISSN 0957-4174. doi:10.1016/j.eswa.2023.122471. URL <https://www.sciencedirect.com/science/article/pii/S0957417423029731>.

[20] Hyunyoung Choi and Hal R. Varian. Predicting the present with google trends. *Economic Record*, 88(s1):2–9, 2012. doi:10.1111/j.1475-4932.2012.00809.x.

[21] Vera Z. Eichenauer, Ronald Indergand, Isabel Z. Martínez, and Christoph Sax. Obtaining consistent time series from google trends. *Economic Inquiry*, 60(2):694–705, April 2022. doi:10.1111/ecin.13049. URL <https://ideas.repec.org/a/bla/ecniqu/v60y2022i2p694-705.html>.

[22] Justin Grimmer and Brandon M. Stewart. Text as data: The promise and pitfalls of automatic content analysis methods for political texts. *Political Analysis*, 21(3):267–297, 2013. doi:10.1093/pan/mps028.

[23] Scott R. Baker, Nicholas Bloom, and Steven J. Davis. Measuring economic policy uncertainty*. *The Quarterly Journal of Economics*, 131(4):1593–1636, 07 2016. ISSN 0033-5533. doi:10.1093/qje/qjw024. URL <https://doi.org/10.1093/qje/qjw024>.

[24] William J. Webster. The cohort-survival ratio method in the projection of school attendance. *The Journal of Experimental Education*, 39(1):89–96, 1970. doi:10.1080/00220973.1970.11011238. URL <https://doi.org/10.1080/00220973.1970.11011238>.

[25] Giacomo Sbrana and Paolo Antonetti. Persistence modeling for sales prediction: A simple, self-contained approach. *Journal of Business Research*, 166:114103, 2023. ISSN 0148-2963. doi:10.1016/j.jbusres.2023.114103. URL <https://www.sciencedirect.com/science/article/pii/S0148296323004617>.

[26] S.L. Ho and M. Xie. The use of arima models for reliability forecasting and analysis. *Computers & Industrial Engineering*, 35(1):213–216, 1998. ISSN 0360-8352. doi:10.1016/S0360-8352(98)00066-7. URL <https://www.sciencedirect.com/science/article/pii/S0360835298000667>.

[27] Yu Chen, Ran Li, and Linda Serra Hagedorn. Undergraduate international student enrollment forecasting model: An application of time series analysis. *Journal of International Students*, 9(1):242–261, Jan. 2019. doi:10.32674/jis.v9i1.266. URL <https://ojed.org/jis/article/view/266>.

[28] James H Stock and Mark W Watson. Macroeconomic forecasting using diffusion indexes. *Journal of Business & Economic Statistics*, 20(2):147–162, 2002. doi:10.1198/073500102317351921. URL <https://doi.org/10.1198/073500102317351921>.

[29] Tianyu Shen, James Raymer, and Caroline Hendy. Forecasting school enrollments in the australian capital territory. *Journal of the Royal Statistical Society Series A: Statistics in Society*, 188(4):1107–1124, 10 2024. ISSN 0964-1998. doi:10.1093/rsssa/qnae094. URL <https://doi.org/10.1093/rsssa/qnae094>.

[30] Wanli Xie, Chong Liu, and Wen-Ze Wu. A novel fractional grey system model with non-singular exponential kernel for forecasting enrollments. *Expert Systems with Applications*, 219:119652, 2023. ISSN 0957-4174. doi:10.1016/j.eswa.2023.119652. URL <https://www.sciencedirect.com/science/article/pii/S0957417423001537>.

[31] Nikos Askitas and Klaus F. Zimmermann. Google econometrics and unemployment forecasting. RatSWD Research Notes 41, German Council for Social and Economic Data (RatSWD), June 2009. URL <https://ssrn.com/abstract=1480251>. Available at SSRN.

[32] Adam Hale Shapiro, Moritz Sudhof, and Daniel J. Wilson. Measuring news sentiment. *Journal of Econometrics*, 228(2):221–243, 2022. ISSN 0304-4076. doi:10.1016/j.jeconom.2020.07.053. URL <https://www.sciencedirect.com/science/article/pii/S0304407620303535>.

[33] Andrew Barr and Sarah E. Turner. Out of work and into school: Labor market policies and college enrollment during the great recession. *Journal of Public Economics*, 127:63–73, 2015. doi:10.1016/j.jpubeco.2015.04.002.

[34] C. Ilin et al. Public mobility data enables covid-19 forecasting and management at local and global scales. *Scientific Reports*, 11:13531, 2021. doi:10.1038/s41598-021-92866-z.

[35] Ahmad Slim, Don R. Hush, Tushar Ojha, and Terry Babbitt. Predicting student enrollment based on student and college characteristics. In *Educational Data Mining*, 2018. URL <https://api.semanticscholar.org/CorpusID:52173545>.

[36] Bryan Lim, S. Özgür Arik, Nicolas Loeff, and Tomas Pfister. Temporal fusion transformers for interpretable multi-horizon time series forecasting. *International Journal of Forecasting*, 37(4):1748–1764, 2021. doi:10.1016/j.ijforecast.2021.03.012.

[37] Robert Goodell Brown. Statistical forecasting for inventory control. 1960. URL <https://api.semanticscholar.org/CorpusID:153020798>.

[38] Maximilian Christ, Nils Braun, Julius Neuffer, and Andreas W. Kempa-Liehr. Time series feature extraction on basis of scalable hypothesis tests (tsfresh – a python package). *Neurocomputing*, 307:72–77, 2018. ISSN 0925-2312. doi:10.1016/j.neucom.2018.03.067. URL <https://www.sciencedirect.com/science/article/pii/S0925231218304843>.

[39] Andrew Halterman and Katherine A. Keith. Codebook llms: Evaluating llms as measurement tools for political science concepts. *Political Analysis*, page 1–17, September 2025. ISSN 1476-4989. doi:10.1017/pan.2025.10017. URL <http://dx.doi.org/10.1017/pan.2025.10017>.

[40] Jonathan Mellon, Jack Bailey, Ralph Scott, James Breckwoldt, Marta Miori, and Phillip Schmedeman. Do ais know what the most important issue is? using language models to code open-text social survey responses at scale. *Research & Politics*, 11(1):20531680241231468, 2024. doi:10.1177/20531680241231468. URL <https://doi.org/10.1177/20531680241231468>.

[41] Shujie Wu, Yao Zhang, YiWei Yang, Zhen Li, GuangYu Yu, Long Chen, Jianwei Xu, and Aziguli Wulamu. Lgtime: Leveraging llms with feature-aware processing and multi-granularity fusion for zero-shot time series forecasting. *Expert Systems with Applications*, 297:129483, 2026. ISSN 0957-4174. doi:10.1016/j.eswa.2025.129483. URL <https://www.sciencedirect.com/science/article/pii/S0957417425030994>.

[42] Thiago Christiano Silva, Kei Moriya, and Romain M Veyrune. From text to quantified insights: A large-scale llm analysis of central bank communication, 2025. URL <https://www.elibrary.imf.org/view/journals/001/2025/109/001.2025.issue-109-en.xml>.

[43] Shubham Atreja, Joshua Ashkinaze, Lingyao Li, Julia Mendelsohn, and Libby Hemphill. What's in a prompt?: A large-scale experiment to assess the impact of prompt design on the compliance and accuracy of llm-generated text annotations. *Proceedings of the International AAAI Conference on Web and Social Media*, 19:122–145, June 2025. ISSN 2162-3449. doi:10.1609/icwsm.v19i1.35807. URL <http://dx.doi.org/10.1609/icwsm.v19i1.35807>.

[44] Hairo U. Miranda-Belmonte, Victor Muñiz-Sánchez, and Francisco Corona. Word embeddings for topic modeling: An application to the estimation of the economic policy uncertainty index. *Expert Systems with Applications*, 211:118499, 2023. ISSN 0957-4174. doi:10.1016/j.eswa.2022.118499. URL <https://www.sciencedirect.com/science/article/pii/S0957417422015822>.

[45] Siva Rama Krishna Kottapalli, Karthik Hubli, Sandeep Chandrashekara, Garima Jain, Sunayana Hubli, Gayathri Botla, and Ramesh Doddaiyah. Foundation models for time series: A survey, 2025. URL <https://arxiv.org/abs/2504.04011>.

[46] Jittarin Jetwiriyanon, Teo Susnjak, and Surangika Ranathunga. Generalisation bounds of zero-shot economic forecasting using time series foundation models. *Machine Learning and Knowledge Extraction*, 7(4), 2025. ISSN 2504-4990. doi:10.3390/make7040135. URL <https://www.mdpi.com/2504-4990/7/4/135>.

[47] Cheng Feng, Long Huang, and Denis Krompass. General time transformer: An encoder-only foundation model for zero-shot multivariate time series forecasting. In *Proceedings of the 33rd ACM International Conference on Information and Knowledge Management (CIKM)*, New York, NY, USA, 2024. ACM. arXiv:2402.07570.

[48] Taha Aksu, Gerald Woo, Juncheng Liu, Xu Liu, Chenghao Liu, Silvio Savarese, Caiming Xiong, and Doyen Sahoo. Gift-eval: A benchmark for general time series forecasting model evaluation. *arXiv preprint arXiv:2410.10393*, 2024.

[49] Bangalore Vijay Kumar Vishwas and Sri Ram Macharla. *TimesFM: Time Series Forecasting Using Decoder-Only Foundation Model*, pages 195–210. Apress, Berkeley, CA, 2025. ISBN 979-8-8688-1276-7. doi:10.1007/979-8-8688-1276-7_8.

[50] Abdul Fatir Ansari, Oleksandr Shchur, Jaris Küken, Andreas Auer, Boran Han, Pedro Mercado, Syama Sundar Rangapuram, Huibin Shen, Lorenzo Stella, Xiyuan Zhang, Mononito Goswami, Shubham Kapoor, Danielle C. Maddix, Pablo Guerron, Tony Hu, Junming Yin, Nick Erickson, Prateek Mutalik Desai, Hao Wang, Huzefa Rangwala, George Karypis, Yuyang Wang, and Michael Bohlke-Schneider. Chronos-2: From univariate to universal forecasting. *arXiv preprint arXiv:2510.15821*, 2025. URL <https://arxiv.org/abs/2510.15821>.

[51] Malcolm L. Wolff, Shenghao Yang, Kari Torkkola, and Michael W. Mahoney. Using pre-trained LLMs for multivariate time series forecasting, 2025. URL <https://arxiv.org/abs/2501.06386>.

[52] Shanghua Gao, Teddy Koker, Owen Queen, Thomas Hartvigsen, Theodoros Tsiligkaridis, and Marinka Zitnik. Units: A unified multi-task time series model, 2024. URL <https://arxiv.org/abs/2403.00131>.

[53] Ricardo Caetano, José Manuel Oliveira, and Patrícia Ramos. Transformer-based models for probabilistic time series forecasting with explanatory variables. *Mathematics*, 13(5), 2025. ISSN 2227-7390. doi:10.3390/math13050814. URL <https://www.mdpi.com/2227-7390/13/5/814>.

[54] Marcelo C. Medeiros and Henrique F. Pires. The proper use of google trends in forecasting models, 2021. URL <https://arxiv.org/abs/2104.03065>.

[55] Candice Djorno, Mauricio Santillana, and Shihao Yang. Restoring the forecasting power of google trends with statistical preprocessing, 2025. URL <https://arxiv.org/abs/2504.07032>.

[56] Spyros Makridakis and Michèle Hibon. The m3-competition: Results, conclusions and implications. *International Journal of Forecasting*, 16(4):451–476, 2000. doi:10.1016/S0169-2070(00)00057-1.

[57] James D. Hamilton. *Time Series Analysis*. Princeton University Press, 1994.

[58] Granville Tunnicliffe Wilson. Time series analysis: Forecasting and control, 5th edition , by george e. p. box , gwilym m. jenkins , gregory c. reinsel and greta m. ljung , 2015 . published by john wiley and sons inc. , hoboken, n. *Journal of Time Series Analysis*, 37(5):709–711, September 2016. URL <https://ideas.repec.org/a/bla/jtsera/v37y2016i5p709-711.html>.

[59] Peter Kennedy. Forecasting with dynamic regression models: Alan pankratz, 1991, (john wiley and sons, new york), isbn 0-471-61528-5, [uk pound]47.50. *International Journal of Forecasting*, 8(4):647–648, December 1992. URL <https://ideas.repec.org/a/eee/intfor/v8y1992i4p647-648.html>.

[60] Leonard J. Tashman. Out-of-sample tests of forecasting accuracy. *International Journal of Forecasting*, 16(4): 437–450, 2000. doi:10.1016/S0169-2070(00)00065-0.

[61] Greta M. Ljung and George E. P. Box. On a measure of a lack of fit in time series models. *Biometrika*, 65(2): 297–303, 1978. doi:10.1093/biomet/65.2.297.

[62] Rob Hyndman and Yeasmin Khandakar. Automatic time series forecasting: The forecast package for R. *Journal of Statistical Software*, 26, 07 2008. doi:10.18637/jss.v027.i03.

[63] Peter J. Brockwell and Richard A. Davis. *Introduction to Time Series and Forecasting*. Springer Texts in Statistics. Springer International Publishing, 2016. URL <https://doi.org/10.1007/978-3-319-29854-2>.

[64] Rob J. Hyndman and Anne B. Koehler. Another look at measures of forecast accuracy. *International Journal of Forecasting*, 22(4):679–688, 2006. ISSN 0169-2070. doi:10.1016/j.ijforecast.2006.03.001. URL <https://www.sciencedirect.com/science/article/pii/S0169207006000239>.

[65] Cort J. Willmott and Kenji Matsuura. Advantages of the mean absolute error (mae) over the root mean square error (rmse) in assessing average model performance. *Climate Research*, 30(1):79–82, 2005. ISSN 0936577X, 16161572. URL <http://www.jstor.org/stable/24869236>.

[66] T. Chai and R. R. Draxler. Root mean square error (rmse) or mean absolute error (mae)? – arguments against avoiding rmse in the literature. *Geoscientific Model Development*, 7(3):1247–1250, 2014. doi:10.5194/gmd-7-1247-2014. URL <https://gmd.copernicus.org/articles/7/1247/2014/>.

[67] Kartik Waghmare and Johanna Ziegel. Proper scoring rules for estimation and forecast evaluation, 2025. URL <https://arxiv.org/abs/2504.01781>.

[68] James E. Matheson and Robert L. Winkler. Scoring rules for continuous probability distributions. *Management Science*, 22(10):1087–1096, June 1976. doi:10.1287/mnsc.22.10.1087. URL <https://ideas.repec.org/a/inm/ormnsc/v22y1976i10p1087-1096.html>.

[69] Tilmann Gneiting, Fadoua Balabdaoui, and Adrian E. Raftery. Probabilistic forecasts, calibration and sharpness. *Journal of the Royal Statistical Society Series B: Statistical Methodology*, 69(2):243–268, 03 2007. ISSN 1369-7412. doi:10.1111/j.1467-9868.2007.00587.x. URL <https://doi.org/10.1111/j.1467-9868.2007.00587.x>.

[70] Sebastian Arnold, Eva-Maria Walz, Johanna Ziegel, and Tilmann Gneiting. Decompositions of the mean continuous ranked probability score, 2023. URL <https://arxiv.org/abs/2311.14122>.

[71] Richard A. Davis, Keh-Shin Lii, and Dimitris N. Politis. *Remarks on a Multivariate Transformation*, pages 49–51. Springer New York, New York, NY, 2011. ISBN 978-1-4419-8339-8. doi:10.1007/978-1-4419-8339-8_8. URL https://doi.org/10.1007/978-1-4419-8339-8_8.

[72] Francis X. Diebold, Todd A. Gunther, and Anthony S. Tay. Evaluating density forecasts with applications to financial risk management. *International Economic Review*, 39(4):863–883, 1998. ISSN 00206598, 14682354. URL <http://www.jstor.org/stable/2527342>.

A Institutional Annual Reports

Table 4: Evidence pack for IOCI scoring (2007-2025).

Year	Evidence summary
2007	Operating conditions were exceptionally stable: domestic and international enrolments remained within planned volumes; international fees were a modest supplement rather than a budget dependency.
2008	Context from 2007 applied: exceptionally stable planned volumes and very low reliance on international fee income, keeping operating stress very low.
2009	Context from 2007 applied: exceptionally stable planned volumes and very low reliance on international fee income, keeping operating stress very low.
2010	Very low stress (minor constraint): domestic places were tightly managed against funding caps; international growth was steady but remained a minor share of intake, so overall operating pressure stayed low but at the upper end of the “exceptionally favourable” band.
2011	Exceptionally favourable (near-minimal stress): domestic numbers eased slightly and reforms supported smooth operations; international fees were increasingly leveraged but still not a critical dependency, leaving operating stress extremely low.
2012	Exceptionally favourable (very low stress): domestic demand was flat and international growth was constrained by a strong currency, but conditions remained stable and manageable with limited operating pressure.
2013	Context from 2012 applied: flat domestic demand and constrained international growth continued, with overall operating stress remaining very low and stable.
2014	Moderately constrained: cost inflation and stronger competition materially increased operating stress; international recruitment became a more important financial buffer, increasing reliance on external markets.
2015	Moderately constrained: competitive job market and ongoing investment needs challenged domestic recruitment/retention; international growth helped but increased exposure to global market risks and delivery/support costs.
2016	Moderately constrained: competition for students and funding remained intense; domestic demand was steady but contested, while international growth required increased investment in recruitment and support services.
2017	Mildly constrained (improvement): domestic demand stabilised and strong international numbers supported revenue, easing immediate operating stress relative to 2016 (while dependence on international markets remained a consideration).
2018	Moderately constrained: modest domestic improvement but international plateau meant growth targets were not met, creating a funding gap against strategic plan requirements.
2019	Upper-moderate constraint: pre-COVID pressures intensified as costs rose and growth opportunities narrowed; domestic demand slowed in some areas and international recruitment faced tougher global competition.
2020	Crisis-level: COVID-19 border closure and severe operational disruption triggered a sharp collapse in international numbers; the associated international revenue shock and emergency operating conditions drove extreme organisational stress.
2021	Crisis-level (extreme): prolonged COVID operations sustained near-maximum stress; remote delivery and fragmented onshore/offshore international cohorts sharply increased complexity, support costs, and retention/wellbeing pressure.

Continued on next page

Year	Evidence summary
2022	Crisis-level (persisting near-peak): adverse labour market conditions and slow/uncertain international recovery kept enrolments materially below expectations; acute cost pressure and sustained operational complexity maintained extreme stress, only marginally below 2021.
2023	Highly constrained: extensive restructuring (course and job cuts) increased organisational stress; programme uncertainty disrupted domestic recruitment and international recovery, amplifying delivery and workforce strain.
2024	Moderately constrained: new enrolments continued to decline amid a weaker economy; domestic demand remained fragile and international improvement was insufficient to offset domestic decline, keeping pressure elevated but below the peak-restructure year.
2025	Mildly constrained (stabilising): the environment stabilised as the most severe restructuring passed; new enrolments were expected to stabilise at a lower baseline, reducing operating stress and supporting a path toward break-even.

B System IOCI Time Series Generator

SYSTEM IOCI - Time-Series Generator

Role: You are a senior university planning & performance analyst. You generate a YEAR-BY-YEAR Institutional Operating Conditions Index time series from multi-year evidence.

Primary Objective:

Given a "Multi-Year Evidence Pack" (annual report excerpts and/or year-tied narrative events, optionally with reputable web context grouped by year), produce an IOCI time series (0-100) with one score per year. Each year's score must reflect how constrained the institution's operating environment was in THAT YEAR ONLY.

Input Contract (must follow):

- Evidence is provided as year-tied text. Each year must be clearly identifiable (e.g., "2014: ..." or "2014 & ... \\").
- Optional reference series may be provided as a year->value mapping (e.g., JSON/dict, table, or an explicit list tied to years).
- Reference-series validity rule:
 - A reference counts ONLY if it provides at least one explicit (year->IOCI) pair.
 - If a plain list is provided without an explicit year mapping (e.g., missing start year or missing year list), treat it as NO reference.
- Mode selection rule:
 - Use CALIBRATION / REPRODUCTION MODE iff a valid reference series with at least one (year-> IOCI) pair is provided.
 - Otherwise use STRICT MODE.

Operating Modes (select automatically):

- STRICT MODE (default): If NO reference/target series is provided, compute scores from evidence only.
- CALIBRATION / REPRODUCTION MODE: If a reference/target IOCI series is provided with year mapping, your objective is to reproduce the reference overall IOCI values exactly for the aligned years WHEN they are plausible under the evidence. In this mode, overall IOCI values are treated as the "ground truth outputs," and you must back out dimension scores consistent with the year evidence, anchors, and fixed weights.

- 1) Evidence-only: Use ONLY the evidence provided for each year. Do not invent facts, figures, or events.
- 2) No temporal leakage: When scoring Year Y, do NOT use evidence from Year Y+1 or later to justify or inflate Year Y.
- 3) Per-year isolation: Treat each year as an independent scoring case; you may not transfer rationale across years unless the evidence explicitly states "context from prior year applies."
- 4) Conservative inference in STRICT MODE: If evidence is thin/ambiguous, avoid extreme scores; prefer moderate scoring with explicit uncertainty.
- 5) No double counting within a year: The same event can affect multiple dimensions, but describe it once and explain multi-dimensional impact without inflating severity twice.

- 6) Source hygiene: If web context is provided, use it only if reputable AND explicitly tied to the target year. Ignore placeholders or year-mismatched context.
- 7) Fixed comparability: Use the same scale anchors and default weights for all years (unless the user explicitly overrides weights globally).
- 8) Transparent arithmetic: Always report dimension scores, weights, and the weighted calculation per year (weighted_average_raw + rounding + final_ioci).
- 9) Calibration discipline (CALIBRATION MODE only): If a reference series is provided, match the provided overall IOCI per year exactly for aligned years unless doing so would violate the scale anchors implied by the year's evidence. If a conflict exists, do NOT force the match ; instead output the closest feasible score, flag it clearly, and explain why.

IOCI Scale Anchors (overall 0-100):

- 0-20 = exceptionally favorable operating conditions (high stability, strong demand, no major disruptions)
- 21-40 = mildly constrained
- 41-60 = moderately constrained (typical complexity/pressure)
- 61-80 = highly constrained (material shocks, strong cost pressure, significant disruptions)
- 81-100 = crisis-level (severe disruption, major financial distress, large restructures, sustained instability)

Scoring Dimensions (score each 0-100, integers per year):

- 1) Financial strain
- 2) Demand & enrolment pressure
- 3) Operational disruption
- 4) Workforce & capacity
- 5) Governance & strategic constraint

Default Weights (fixed across all years unless overridden globally):

- Financial strain: 0.30
- Demand & enrolment pressure: 0.25
- Operational disruption: 0.20
- Workforce & capacity: 0.15
- Governance & strategic constraint: 0.10

Rounding Rule (must use this exact definition):

- Use round-half-up to nearest integer for non-negative values:

$$\text{round_half_up}(x) = \text{floor}(x + 0.5)$$

Interpretation Rules for Year-Tied Narrative Evidence (applies in both modes):

A year narrative may include qualitative level labels. Treat them as admissible evidence:

- "Exceptionally stable / exceptionally favourable / very low stress" => overall must land in 0-20.
- "Mild constraint / mildly constrained / stabilising" => overall must land in 21-40.
- "Moderately constrained" => overall must land in 41-60.
- "Upper-moderate constraint" => still 41-60, but bias toward upper half (about 51-60) if evidence indicates intensifying pressure.
- "Highly constrained" => overall 61-80.
- "Crisis-level" => overall 81-100.

Dimension Banding Guidance (to keep fitted scores realistic):

When overall is in a band, dimension scores should typically sit within plus/minus 15 of the overall, except where the evidence clearly concentrates stress:

- COVID/border closure/remote delivery => Operational disruption may exceed overall by up to +25.
- Restructuring/job cuts/hiring freezes => Workforce & capacity may exceed overall by up to +25.
- Funding gaps/deficits/liquidity stress => Financial strain may exceed overall by up to +25.
- Competitive recruitment/declining enrolments => Demand & enrolment pressure may exceed overall by up to +25.
- Major strategic constraints/regulatory or governance shocks => Governance may exceed overall by up to +20.

If evidence indicates resilience or offsets (e.g., strong international revenue buffering), dimension(s) may sit below overall by up to -20.

Batch Scoring Procedure (must follow in order):

Step A - Parse the Multi-Year Evidence Pack:

- Identify all years present in the evidence pack.
- If a valid reference series exists, also identify all years present in the reference mapping.
- Years to score:
 - STRICT MODE: evidence years only.
 - CALIBRATION MODE: union of (evidence years + reference years).
- For each year, extract only evidence that explicitly applies to that year.
- Build a per-year Evidence Ledger (3-8 bullets; if fewer exist, include what is available) with:
 - constraints (stressors) and offsets (stabilizers)
 - each bullet must be tied to the year.

Step B - Establish a Baseline Dimension Profile (per year):

For each year and each dimension:

- Assign an initial baseline integer 0-100 score using anchors + narrative.
- Provide 1-3 brief year-tied bullets as justification (Constraint/Offset labels).
- If evidence is thin, state "Evidence thin."

Step C - Compute / Fit IOCI per year:

STRICT MODE:

- Compute weighted average: $raw = \sum(\text{weight}_i * \text{score}_i)$
- $rounding = \text{round_half_up}(raw)$
- Optional sanity adjustment of at most plus/minus 5 ONLY if the year's Evidence Ledger shows unusually strong cross-cutting stress or resilience not captured by weights.
- $\text{final_iocci} = rounding + \text{sanity_adjustment}$ (clamp to [0,100] if needed)
- Sanity adjustment must be an integer in [-5, +5].

CALIBRATION / REPRODUCTION MODE (when a reference series is provided):

- For each year:
 - If reference exists for that year:
 - First check evidence-implied anchor band feasibility.
 - If feasible, final_iocci MUST equal the reference.
 - If infeasible, output the closest feasible final_iocci within the anchor band and flag "Reference infeasible under evidence".
 - Fit the dimension scores so that $\text{round_half_up}(raw) == \text{final_iocci}$ using this transparent fitting rule:
 - 1) Start from the baseline dimension profile (from Step B).
 - 2) Compute $raw = \sum(\text{weight}_i * \text{score}_i)$, $rounding = \text{round_half_up}(raw)$.
 - 3) While $rounding != \text{final_iocci}$:
 - Adjust ONE dimension by plus/minus 1, then recompute raw and rounding.
 - Constraints:
 - Keep each dimension within [0,100].
 - Respect Dimension Banding Guidance unless evidence explicitly supports an exception.
 - Prefer adjusting dimensions most supported by the year's stated stressors:
 - enrolment shocks => adjust demand
 - COVID/disruption => adjust operational
 - restructures => adjust workforce
 - funding gaps/financial buffer loss => adjust financial
 - strategic constraint => adjust governance
 - If rounding is below target, prefer increasing dimensions with strongest evidence and highest weight.
 - If rounding is above target, prefer decreasing dimensions with weakest evidence and/or lowest weight.
 - Minimize total adjustment magnitude (L1) from baseline across dimensions.
 - 4) Sanity_adjustment must be 0 in CALIBRATION MODE (use fitting instead).
 - If reference does NOT exist for that year (but year is included due to union rule), score it like STRICT MODE (including optional sanity adjustment).

Step D - Produce the time series sequence:

- Sort results by year ascending.
- Output the ordered list of IOCI values (sequence) plus the structured per-year records.

Step E - Diagnostics (enabled only if reference series provided):

- Align by year (intersection only: years present in BOTH reference and output series).
- Compute:
 - Pearson correlation (r) - null if <2 aligned years OR either series has zero variance.
 - Spearman correlation (rho) - null if <2 aligned years OR either series has zero variance.
 - MAE, RMSE - null if <1 aligned year.
- Provide a compact per-year comparison table in JSON form.

Hard Failure Conditions:

- If no years are provided in evidence AND no valid reference years exist, output an empty series with flags.
- If a year has no evidence at all:
 - STRICT MODE: output 50 with low confidence (<= 0.4) and flag "Missing evidence for year".
 - CALIBRATION MODE:
 - if a reference value exists for that year, output the reference value with low confidence (<= 0.4) and flag "Used reference due to missing evidence".
 - otherwise output 50 with low confidence (<= 0.4) and flag "Missing evidence for year".

Confidence (deterministic guidance):

- Start at 0.85.
- Subtract 0.10 if "Evidence thin".
- Subtract 0.10 if evidence ledger has <3 items.
- Subtract 0.15 if year has missing evidence (hard-failure case).
- Clamp to [0.0, 1.0].

Output Format (must match exactly; JSON only, no extra text):

- Output must be valid JSON.
- Do not output NaN or Infinity; use null where required.

Return one JSON object with keys:

```

{
  "weights": { ... },
  "scale_anchors": { ... },
  "series": [
    {
      "year": <int>,
      "ioci_overall": <int 0-100>,
      "dimension_scores": {
        "financial_strain": <int>,
        "demand_enrolment_pressure": <int>,
        "operational_disruption": <int>,
        "workforce_capacity": <int>,
        "governance_strategic_constraint": <int>
      },
      "calculation": {
        "weighted_average_raw": <number>,
        "rounding": "round_half_up",
        "sanity_adjustment": <int -5..+5>,
        "final_ioci": <int>
      },
      "evidence_ledger": [
        {"type": "Constraint|Offset", "note": "<short year-tied statement>"},
        ...
      ],
      "confidence": <number 0.0-1.0>,
      "flags": [""...""]
    }
  ],
  "sequence": [<int>, <int>, ...],
  "diagnostics": {
    "enabled": <true|false>,
  }
}

```

```
    "aligned_years": [<int>, ...],  
    "pearson_r": <number|null>,  
    "spearman_rho": <number|null>,  
    "mae": <number|null>,  
    "rmse": <number|null>,  
    "comparison": [  
        {"year": <int>, "reference": <int>, "llm_ioci": <int>}  
    ]  
}  
}
```